

# Rare Earth Element and Yttrium Variability in South East Queensland Waterways

MICHAEL G. LAWRENCE, ALAN GREIG, KENNETH D. COLLERSON and BALZ S. KAMBER

*Advanced Centre for Queensland University Isotopic Research Excellence, University of Queensland, Richards Building, Brisbane, QLD 4072, Australia*

Received 14 September 2004; accepted 22 March 2005

**Abstract.** We present data for the rare earth elements and yttrium (REY) in the National Research Council of Canada natural river water reference material SLRS-4 and 19 natural river waters from small catchments in South-East Queensland, Australia, by a direct ICP-MS method. The 0.22  $\mu\text{m}$  filtered river water samples show a large degree of variability in both the REY concentration, e.g., La varies from 13 to 1157 ppt, and shape of the alluvial-sediment-normalised REY patterns with different samples displaying light, middle or heavy rare earth enrichment. In addition, a spatial study was undertaken along the freshwater section of Beerburum Creek, which demonstrates that  $\sim 75\%$  of the total REYs in this waterway are removed prior to estuarine mixing without evidence of fractionation.

**Key words:** fractionation, ICP-MS, Queensland, rare earth elements, rivers, SLRS-4, yttrium

## 1. Introduction

The rare earth elements and yttrium (REE when discussed without Y or REY when included) are extremely useful geochemical proxies as the changes in atomic structure across the series vary predictably, and in much smaller increments than any other group of elements. Geochemical study of REE distribution spans decades and results obtained have answered many important biogeochemical questions (Goldberg et al., 1963; Elderfield, 1988; Piepgras and Jacobsen, 1992; Sholkovitz, 1992, 1995; Zhang and Nozaki, 1996; Lerche and Nozaki, 1998; Nozaki et al., 2000a, b; Astrom, 2001; Nelson et al., 2003; Runnalls and Coleman, 2003; Wyndham et al., 2004).

Many of the earlier studies of REE distribution in river, estuarine and oceanic waters were conducted using isotope dilution – a highly precise method for polyisotopic REE but incapable of analysis of the 5 mono-isotopic REE (Hoyle et al., 1984; Elderfield, 1988; Sholkovitz et al., 1989; 1999; Sholkovitz, 1992; 1995). These studies have provided the majority of the REE data currently in the aquatic chemistry literature, and have provided the foundation for our understanding of aquatic REE chemistry. Not

withstanding these achievements, thermal ionisation (ID-TIMS) techniques are not applicable to all geochemical questions due to the requirement for large sample volumes, lengthy analysis times, and an inability to determine the monoisotopic REE and Y. It is now clear that some of the anomalies that uniquely typify the marine REY pattern cannot be accurately quantified, or fully appreciated, without data for at least some of the monoisotopic REE's and Y. The 'unique' features that characterise marine REY patterns relative to shale include: a strong light REE (LREE) depletion, a strong positive La anomaly, a strong negative Ce anomaly, a variable Eu anomaly, a small positive Gd anomaly and a strong overenrichment of Y relative to its chemical 'twin' Ho e.g., Alibo and Nozaki (1999). Whilst all these typically 'marine' features can be recognised in complete REY datasets in seawater, the origin of 'anomalous' abundances remains contentious (Masuda and Ikeuchi, 1979; Masuda and Shimoda, 1997). A number of important questions regarding the origins of the marine REY anomalies, and hence the overall marine REY pattern, are still to be resolved. Are the features genuinely the result of marine processes only? Can the features develop in freshwater, and subsequently be transferred to saline waters? Do the features develop as a consequence of processes occurring within the estuarine trap?

The observational and experimental evidence presently available (Elderfield et al., 1990; Byrne and Sholkovitz, 1996) is inconclusive. Furthermore, the mixing experiment of Hoyle et al. (1984) does not reproduce the anomalies typically associated with the marine REE pattern, although the data presented are difficult to evaluate partly due to the lack of monoisotopic element data, and additionally due to the choice of filtration parameters.

The situation is compounded by the surprising paucity of complete REY data for freshwater. In fact, we are unaware of any publication that presents a spatial analysis of the natural behaviour of the complete set of REY in the freshwater regime of any river. It is therefore impossible, within the constraints of existing datasets, to evaluate the mechanisms for generating seawater REY features, because the specific behaviour of REYs in freshwater and during estuarine mixing is not well established. This fact was previously noted by Byrne and Liu (1998) who stated (p. 119) "Clearly, an improved understanding of riverine fractionation processes appears essential to better constrain the comparative fractionation or YREEs in riverine/estuarine systems and seawater".

Recently, the question about the significance and origin of the marine dissolved REY abundance has attracted renewed attention as hydrogenous sediments (chert, iron oxide, carbonate) appear to preserve marine REY features as far back as 3.71 Ga (Kamber and Webb, 2001; Van Kranendonk et al., 2003; Bolhar et al., 2004; Nothdurft et al., 2004). If confirmed, these findings imply an extraordinary resilience of REY fractionation processes through Earth's history (Shields and Webb, 2004). Indeed, given that the

oceanic residence times of REYs are in the range of hundreds to thousands of years, one cannot fail to be impressed by the longevity of the marine REY signature.

In order to address the question of the origin of the marine REY fingerprint we have developed here, as a preparatory step, an extensive REY dataset for river and slightly saline waters from South East Queensland using an ICP-MS technique capable of directly quantifying all 15 naturally occurring REY. Our study demonstrates a remarkable variability in REY abundance in river water from a relatively small region, which suggests that REY have the potential to be used as a source fingerprint. Furthermore, the data demonstrate that certain typical ‘marine’ REY features appear to develop in essentially fresh river waters, prior to entering the estuarine trap.

## 2. Sample Location and Collection

The subtropical South-East region of Queensland is the most densely populated area of the state (home to ~65% of the state’s population, although only comprising 1.5% of the total land area). Many of the waterways of the region drain into Moreton Bay, an anthropogenically impacted coastal embayment currently attracting significant scientific interest in an effort to improve water quality (Abal et al., 2001). We obtained our samples from 19 waterways in three field trips (Figure 1) as described below.

The first samples were obtained from the Gold Coast region, sampling the Nerang and Coomera Rivers in upstream and downstream locations, and Tallebudgera and Currumbin Creeks. The catchments sampled all drain a geologically similar mountainous hinterland that is largely basaltic, with significant areas of remnant native vegetation and smaller rural residential areas (Willmott, 2004). The initial samples were filtered with both 0.45 and 0.22  $\mu\text{m}$  filters to allow determination of fractionation introduced by filtration. Following evaluation of the results (Section 5.1.1), all subsequent samples were filtered at 0.22  $\mu\text{m}$  only.

On the second sampling excursion, we collected waters from 15 additional streams within 100 km to the north of Brisbane (the Sunshine Coast), with a strategy designed to cover a larger range of lithological terrains and land use regions. The geology of these catchments is significantly more complex comprising heavily weathered Tertiary and Quaternary sandstone and siltstones, although some creeks partially drain the Tertiary alkaline intraplate volcanics of the Glass House Mountains (Willmott, 2004).

A third, much more detailed, set of samples was taken in Beerburrum Creek – the waterway previously identified as containing the highest total REY concentration – to determine spatial variations in REY profile and elucidate the mechanisms of fractionation, if any, in this waterway. This creek was identified for a future study of estuarine REY removal.

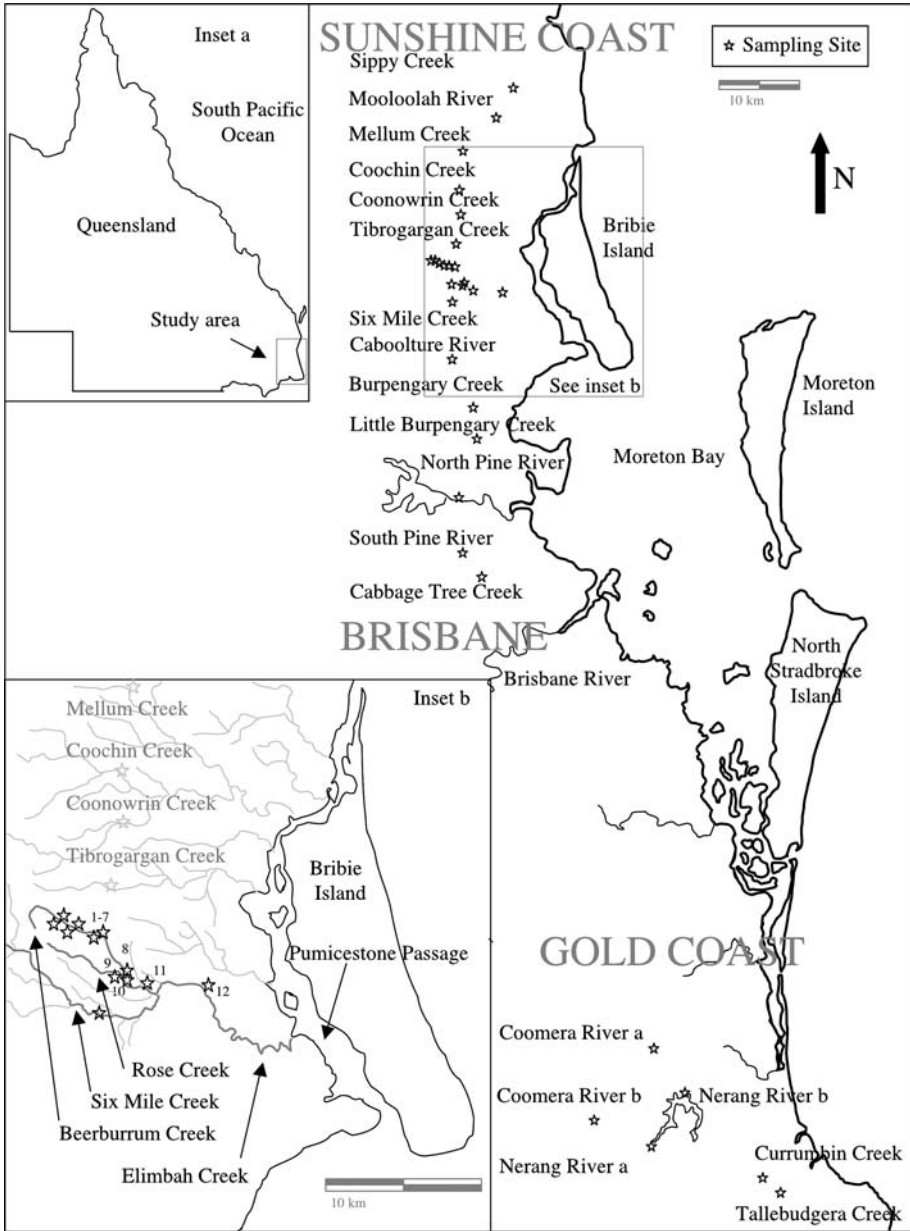


Figure 1. Map of SE Queensland coastline and sampling localities (star symbols). Inset (a) shows study area in relation to the state of Queensland (an area more than 3 times the size of California). Inset (b) shows sites of detailed sampling along Elimbah Creek tributaries.

Depending on stream width and depth at the sampling location, samples were taken either 3 m from the bank, or in midstream at a depth between 5 and 50 cm. Care was taken to avoid surface microlayer effects. Approxi-

mately 12 mL of stream water was filtered through a rinsed Millex HV 0.22  $\mu\text{m}$  syringe filter into pre-weighed and pre-cleaned low-density polyethylene centrifuge tube. Samples were transported back to the laboratory at room temperature, immediately spiked with internal standards, and analysed the same day. The longest time between collection and analysis of any individual sample was 16 hours.

Other parameters recorded for each site included pH, temperature, conductivity and GPS coordinates. Each site was photographed upstream and downstream of the sampling to allow later evaluation of stream and riparian vegetation condition. pH, temperature and conductivity were measured with a TPS meter calibrated with a 2-point calibration for pH in the morning (pH 4 and 6.88), and periodically rechecked with a pH buffer (7). Conductivity was calibrated with a standard at 276 mS prior to leaving the laboratory and periodically through the day.

### 3. Analytical Method

All sample manipulations and analyses were performed within the ACQUIRE laboratory, a 200 m<sup>2</sup> HEPA-filtered, temperature and humidity controlled Class-100 to Class-10,000 clean-room facility (Collerson, 1995). Approximately 12 mL of each water sample was spiked with  $\sim 120 \mu\text{L}$  of 200 ppb internal standard (In, Re, Bi) in 2% HNO<sub>3</sub>, to give a final concentration of 2 ppb in 0.02% HNO<sub>3</sub>. Field and laboratory blanks were prepared for each batch of samples and the N.R.C. river water reference material SLRS-4 was treated as an unknown. Samples were analysed on a Thermo X-Series ICP-MS with a Peltier cooled quartz impact bead spray chamber and a 0.4 mL/min borosilicate nebuliser. A high performance interface cone set was used, delivering instrument sensitivity of approximately 200 MHz/ppm In and 350 MHz/ppm U with a background of  $<0.2$  cps at mass 220. Three points per peak were measured with a spacing of 0.02 a.m.u. and dwell times ranging from 10 to 50 ms. Fifty sweeps constituted one repeat and five repeats were measured for samples and eight for blanks. We analysed the full suite of REYs, Mn, Zr, U and Th and the appropriate interfering isotopes. Interference corrections used oxide and hydroxide production rates of single element standards measured at the completion of the analytical run. Appropriate corrections were applied to all REE including and heavier than Eu.

In contrast to other studies (Shabani et al., 1990; Zhang and Nozaki, 1996; Yeghicheyan et al., 2001), we used a dilute natural rock solution as a calibration standard. First, because of the excellent quality of data available for these standards (e.g., Baker et al., (2002)). Second, preparing a mixed multi-element calibration standard from 'pure' single element REY solutions without cross-contamination is difficult (i.e. at the level desired, the single

element solutions available to us appear to contain other REY, so a combined calibration standard would not be accurate). Third, natural basaltic rocks chosen as geological reference materials have smooth chondrite and shale-normalised REY abundances. Because REY data for waters (and all other materials) are invariably presented as normalised patterns, it is logical to choose a calibration standard with a smooth shale-normalised REY pattern (other than Eu). Fourth, a very dilute rock solution will have a more similar matrix to a natural water sample than a synthetic REY solution.

Two separate digestions of U.S.G.S. dolerite W-2 were used as calibration standards and two other U.S.G.S. basalt reference materials BIR-1 and BHVO-2 were analysed as unknowns. The poly-isotopic REE abundances for these reference materials have been accurately and precisely determined by ID-TIMS and ID-MC-ICP-MS (Raczek et al., 2001; Baker et al., 2002) and mono-isotopic REE can be estimated by interpolation on chondrite normalised REY diagrams assuming they have smooth patterns (Cheatham et al., 1993). Our calibration values are based on published ID-TIMS values for BHVO-1 (Raczek et al., 2001), against which we calibrated W-2. Slight discrepancies for some elements, e.g., Yb, between the two ID techniques is a spike calibration issue (Baker et al., 2002). Our preferred composition for W-2 is shown in Table I.

One hundred milligrams of the reference materials were digested with distilled HF–HNO<sub>3</sub> in Teflon beakers on a hotplate, evaporated to dryness, refluxed with HNO<sub>3</sub> then dissolved in 1.5 N HNO<sub>3</sub>. The standards were diluted in polypropylene bottles and spiked to produce solutions with 2 ppb internal standard concentration and sample dilution factors of 10,000. At this dilution, the REY concentrations of the reference materials are between 5 and 20 times the concentrations expected for NRCC SLRS-4. On our instrument, a 10,000-fold dilution of W-2 yielded count rates on REY isotopes between 13,000 cps with an RSD of 0.141% for <sup>175</sup>Lu and 540,000 cps with an RSD of 0.179% for <sup>140</sup>Ce. RSDs in undiluted SLRS-4 (with lower count rates) were generally less than 1%, but up to 3.8% for <sup>167</sup>Er. Additional geological reference materials (BIR-1 and BHVO-2) at similar dilutions were analysed as unknowns, and the results (Table I) are in excellent agreement with our internal laboratory long-term average and published ID analyses (Raczek et al., 2001; Baker et al., 2002).

External drift correction was achieved by analyses of interspersed (typically every 5–8 samples) drift monitors (Eggins et al., 1997), followed by a blank. A mix of the calibration solutions was diluted a further three times for this purpose. Rock standards were run at the end of the analytical run to prevent carryover. The sample washout routine was 30 s of 0.5% Triton X-100, 140 s of 5% HNO<sub>3</sub>, 70 s of 2% HNO<sub>3</sub>, and 70 s of Milli-Q water. Through the course of these analyses, 17 separate preparations of the reference material SLRS-4 including 10 dilutions from 1:3 to 1:425 were run over five analytical sessions and are presented in Table I.

Table 1. Calibration, published and measured REY concentrations of reference materials used for this study

	La	Ce	Pr	Nd	Sm	Eu	Gd	Tb	Dy	Y	Ho	Er	Tm	Yb	Lu
W-2 preferred values	10521	23216	3025	12911	3266	1094	3708	615	3808	20113	803	2222	327	2058	301
BIR-1 preferred values	600	1901	378	2379	1099	524	1860	363	2538	14532	582	1699	257	1656	247
BHVO-2 preferred values	15113	37518	5373	24332	6071	2051	6222	937	5244	24340	1005	2509	339	2003	274
MUQ (Kamber et al., 2005)	32510	71090	8460	32910	6880	1570	6360	990	5890	31850	1220	3370	510	3250	490
BIR-1 measured	603	1896	377	2372	1086	519	1867	364	2534	14734	581	1691	258	1650	245
BHVO-2 measured	15210	38022	5390	24451	6045	2051	6234	933	5234	24292	999	2517	339	1988	274
SLRS-4 (Yeghicheyan et al., 2001)	0.2870	0.3600	0.0693	0.2690	0.0574	0.0080	0.0342	0.0043	0.0242	not determined	0.0047	0.0134	0.0017	0.0120	0.0019
error (1 sd)	0.0080	0.0120	0.0018	0.0140	0.0028	0.0006	0.0020	0.0004	0.0016		0.0003	0.0006	0.0002	0.0004	0.0001
Undiluted															
SLRS-4 a	0.3049	0.3784	0.0744	0.2803	0.0610	0.0080	0.0343	0.0044	0.0237	0.1336	0.0049	0.0147	0.0019	0.0111	0.0016
SLRS-4 b	0.2949	0.3708	0.0716	0.2712	0.0587	0.0078	0.0345	0.0043	0.0234	0.1295	0.0048	0.0130	0.0019	0.0121	0.0019
SLRS-4 c	0.3091	0.3829	0.0747	0.2781	0.0593	0.0080	0.0353	0.0045	0.0241	0.1424	0.0048	0.0135	0.0019	0.0118	0.0019
SLRS-4 d	0.3044	0.3831	0.0739	0.2778	0.0589	0.0078	0.0352	0.0045	0.0238	0.1431	0.0048	0.0135	0.0019	0.0120	0.0019
SLRS-4 e	0.2982	0.3755	0.0737	0.2764	0.0585	0.0081	0.0351	0.0044	0.0234	0.1452	0.0048	0.0130	0.0019	0.0122	0.0019
SLRS-4 f	0.2922	0.3671	0.0715	0.2704	0.0574	0.0075	0.0343	0.0044	0.0237	0.1315	0.0048	0.0128	0.0019	0.0122	0.0019
SLRS-4 g	0.3119	0.3912	0.0752	0.2874	0.0615	0.0094	0.0372	0.0050	0.0253	0.1367	0.0051	0.0142	0.0020	0.0128	0.0019
Dilutions (SLRS-4/dilution factor)															
SLRS-4/3	0.3125	0.3861	0.0743	0.2837	0.0606	0.0081	0.0351	0.0044	0.0240	0.1424	0.0050	0.0135	0.0020	0.0120	0.0020
SLRS-4/5	0.2943	0.3658	0.0718	0.2697	0.0581	0.0080	0.0324	0.0043	0.0231	0.1375	0.0048	0.0143	0.0019	0.0106	0.0019
SLRS-4/6	0.3126	0.3943	0.0742	0.2793	0.0589	0.0085	0.0358	0.0045	0.0240	0.1434	0.0047	0.0135	0.0019	0.0124	0.0021
SLRS-4/10	0.2933	0.3631	0.0715	0.2753	0.0580	0.0075	0.0329	0.0041	0.0239	0.1399	0.0046	0.0138	0.0018	0.0104	0.0019
SLRS-4/21	0.3059	0.3824	0.0753	0.2725	0.0524	0.0081	0.0313	0.0043	0.0248	0.1322	0.0049	0.0143	0.0020	0.0117	0.0019
SLRS-4/52	0.3039	0.3858	0.0731	0.2709	0.0557	0.0082	0.0317	0.0043	0.0220	0.1342	0.0051	0.0146	0.0020	0.0103	0.0021

Table I. Continued

	La	Ce	Pr	Nd	Sm	Eu	Gd	Tb	Dy	Y	Ho	Er	Tm	Yb	Lu
SLRS-4/72	0.3066	0.3789	0.0717	0.2667	0.0604	0.0074	0.0318	0.0042	0.0258	0.1369	0.0048	0.0138	0.0019	0.0101	0.0019
SLRS-4/105	0.3116	0.3799	0.0723	0.2714	0.0459	0.0058	0.0369	0.0040	0.0231	0.1408	0.0050	0.0130	0.0021	0.0129	0.0020
SLRS-4/212	0.3055	0.3717	0.0725	0.2651	0.0352	0.0083	0.0275	0.0043	0.0171	0.1532	0.0052	0.0138	0.0008	0.0100	0.0018
SLRS-4/425	0.2668	0.3386	0.0682	0.2690	0.0454	0.0011	0.0318	0.0017	0.0380	0.1309	0.0058	0.0097	0.0019	0.0120	0.0026
Average (undiluted)	0.3022	0.3784	0.0736	0.2774	0.0593	0.0081	0.0351	0.0045	0.0239	0.1374	0.0049	0.0135	0.0019	0.0120	0.0019
error (1 sd)	0.1322	0.1641	0.0322	0.1176	0.0253	0.0033	0.0147	0.0018	0.0099	0.0067	0.0020	0.0059	0.0008	0.0051	0.0008

All units in ppb. The data can be retrospectively adjusted by authors who prefer slightly different calibration values for W-2.



## 4. Results

### 4.1. SLRS-4

The N.R.C. reference material SLRS-4 is certified for 22 trace and major elements, but not the REY. However, recently Yeghicheyan et al. (2001) published a comprehensive set of results for the concentrations of REEs for this standard, so that it can be used as an unknown for aquatic REE method development. Readers should be aware that the units in which the REE are reported in that publication were unfortunately mislabelled and should read ng/L not  $\mu\text{g/L}$  (D. Yeghicheyan, 2004, personal communication). The listed data are the combined results of 4 laboratories, 5 techniques and more than 170 analyses of the reference material. The spread of data from these analyses is small, although there are systematic differences, which may reflect the fact that not all laboratories appear to have corrected for certain oxide interferences. Yeghicheyan et al. (2001) suggested that the 'direct' Toulouse values for the heavy REE, (HREE) are lower than other datasets as oxide and hydroxide corrections (Aries et al., 2000) were applied. Nevertheless, our values for undiluted SLRS-4 compare favourably (see Figure 2) to the average presented by Yeghicheyan et al. (2001), with concentrations for all elements agreeing within one standard deviation errors.

### 4.2. DETECTION LIMIT

The sensitivity of the ICP-MS was evaluated for all analysed elements. Here we discuss the results for the monoisotopic Pr and Tm. For both elements

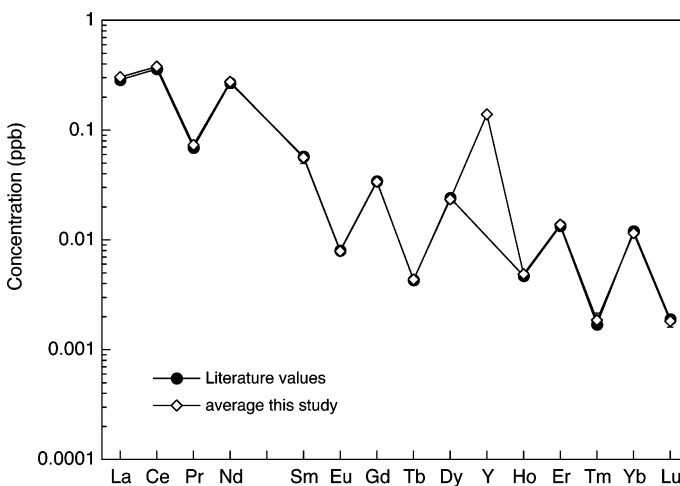


Figure 2. Average (this study) absolute REY concentrations in the NRCC river water reference material SLRS-4 ( $n=9$ ) compared with literature values (Yeghicheyan et al., 2001).

our instrument operating conditions yielded a sensitivity of  $\sim 320$  cps/ppt in solution. Blank levels (estimated from analyses of internal standard spiked 2% double quartz distilled nitric acid in ultra-pure water) were 9 and 1 cps, respectively, for Pr and Tm. If the instrument detection limit is calculated by multiplying the standard deviation of the average blank ( $Tm = 1.03 \pm 0.28$  cps;  $n = 10$ ) by a factor of 3, we obtain 0.84 cps, which at the sensitivity of our instrument translates to 3 ppq (parts per quadrillion, or femtogram per gram). According to this calculation, our instrument detection limit for Tm is reached in SLRS-4 at a dilution factor of  $\sim 600$ . Applying the same reasoning to Pr (blank =  $8.8 \pm 4.8$  cps) results in an instrument detection limit of 14.4 cps, equivalent to 22 ppq. The instrument detection limit is reached for Pr in SLRS-4 with a dilution factor of  $\sim 1000$ .

In order to explore the practicable detection limit of our method, we carried out a series of dilution experiments with SLRS-4. The standard was gravimetrically adjusted to the following dilutions: 3, 5, 6, 10, 21, 52, 72, 104, 212 and 425. The MUQ-normalised (MUQ: a Queensland alluvial sediment average representing a compilation of the sedimentary composition of 25 Queensland rivers Kamber et al., 2005). REY patterns of this dilution series are illustrated in Figure 3. It is evident that the method can be used to reliably determine REE abundances in waters with REE concentrations at least two orders of magnitude lower than SLRS-4. At more extreme dilutions (210 and 425) scatter starts to appear in the pattern. The scatter at high dilutions most likely reflects imperfect blank correction. Further refinement of the method will focus on minimising blank contributions. Nonetheless, it is remarkable that Pr, Nd, Gd, Tm and Yb are still accurately determined at

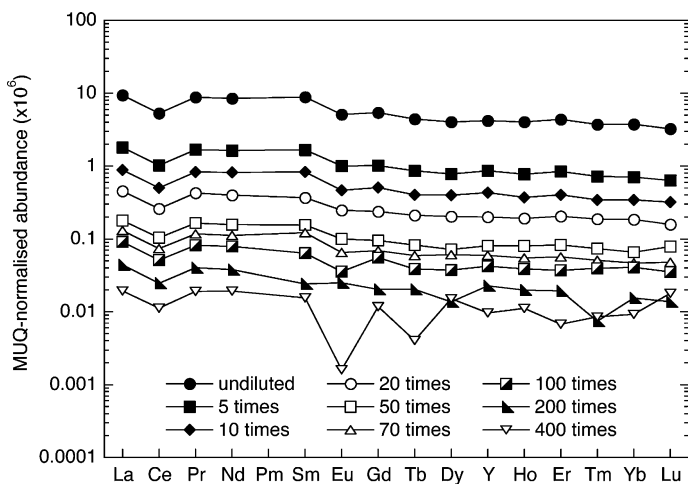


Figure 3. MUQ normalised REY patterns of sequential dilutions of NRCC river water reference material SLRS-4. The retention of the overall REY pattern to at least 100 times dilution is indicative of the exceptional quantification limits of our technique.

425 times dilution, although the result for Tm may be fortuitous as the result obtained for the 210 times dilution is inaccurate. Ultimately, our ability to determine REY concentrations near the detection limit of the instrument is controlled not by the instrumental sensitivity, but by our ability to consistently control the analytical blank near or below single digit ppq levels. This level of performance is only possible due to the environment in which reagents are prepared, and in which the ICP-MS is housed. Practically, for the reference material SLRS-4, our method detection limit is in the range of tens to hundreds of ppq over the complete range of REYs.

### 4.3. SOUTH-EAST QUEENSLAND STREAMS

The rare earth element concentrations of SE Qld streams (Table II) were normalised to a Queensland alluvial sediment average from 25 rivers (MUQ; Kamber et al., 2005.) Whilst there are specific data available for the REY composition of the sediments of three of the studied streams (Tallebudgera Creek, North Pine and Caboolture Rivers; Kamber et al., 2005), it is more instructive to normalise our entire dataset with the more general local sediment average to enable clearer comparisons between datasets. All REY data were blank corrected with field blanks obtained by sampling MilliQ water in the same manner as the samples. Field blanks were spiked with internal standard on return to the laboratory, and analysed as part of the analytical run. The REY content of the field blanks is indistinguishable from internal standard spiked MilliQ water prepared within the clean laboratory.

Comprehensive illustration of REY patterns combines a discussion of overall shape with quantitative expression of anomalies. REE anomalies are calculated as  $REE_n/REE_n^*$  where  $REE_n^*$  is the expected normalised concentration when interpolated from an appropriate combination of near neighbours. Values  $>1$  indicate a positive anomaly and values  $<1$  indicate a negative anomaly. We use the  $Pr_n/Yb_n$  ratio as a general descriptor of the slope of the pattern, with values  $>1$  indicating light enrichment, and values  $<1$  indicating heavy enrichment (neither Pr nor Yb behave anomalously, thus are suitable representative elements). Middle REE enrichments, similar to those described by Shiller (submitted), can be evaluated with  $Pr_n/Tb_n$  and  $Tb_n/Yb_n$ .

Anomaly calculations in aquatic REE are more complicated than in solid geological materials. The principal requirement for calculating anomalies is that the near neighbours used in the calculation must not show any anomalous behaviour themselves. For example, for the calculation of  $La^*$  we cannot use  $Ce_n$  as the oxidation from  $Ce^{3+}$  to  $Ce^{4+}$  often leads to an underabundance of Ce. As a result, La anomalies are calculated using the nearest available non-anomalous REE  $Pr_n$  and  $Nd_n$ . Similarly  $Ce^*$  is also

*Table II.* Rare earth element, yttrium manganese and zirconium concentrations (ppb) for South

Sample Name	La	Ce	Pr	Nd	Sm	Eu	Gd	Tb	Dy
Coomera River b	0.0519	0.0952	0.0150	0.0684	0.0156	0.0030	0.0159	0.0022	0.0135
Coomera River a	0.0376	0.0611	0.0118	0.0546	0.0152	0.0025	0.0164	0.0025	0.0144
Nerang River b	0.0687	0.1100	0.0192	0.0832	0.0195	0.0041	0.0199	0.0030	0.0186
Nerang River a	0.0643	0.1236	0.0200	0.0869	0.0217	0.0038	0.0235	0.0033	0.0204
Tallebudgera Creek	0.0619	0.1177	0.0178	0.0752	0.0158	0.0029	0.0143	0.0021	0.0118
Currumbin Creek	0.0804	0.1633	0.0213	0.0885	0.0184	0.0041	0.0174	0.0025	0.0147
Coomera River b	0.0438	0.0757	0.0123	0.0547	0.0130	0.0025	0.0132	0.0018	0.0102
Coomera River a	0.0320	0.0517	0.0099	0.0453	0.0123	0.0022	0.0141	0.0021	0.0126
Nerang River b	0.0596	0.0938	0.0167	0.0749	0.0176	0.0036	0.0186	0.0027	0.0170
Nerang River a	0.0545	0.1048	0.0172	0.0762	0.0197	0.0034	0.0204	0.0031	0.0176
Tallebudgera Creek	0.0507	0.0980	0.0148	0.0644	0.0133	0.0024	0.0123	0.0017	0.0102
Currumbin Creek	0.0673	0.1329	0.0175	0.0728	0.0150	0.0033	0.0141	0.0020	0.0123
Cabbage Tree Creek	0.1023	0.1400	0.0222	0.0937	0.0198	0.0035	0.0176	0.0025	0.0147
South Pine River	0.0277	0.0470	0.0071	0.0277	0.0059	0.0011	0.0058	0.0008	0.0047
North Pine River	0.0160	0.0249	0.0041	0.0169	0.0042	0.0004	0.0045	0.0006	0.0032
Little Burpengary Creek	0.1731	0.4124	0.0523	0.2244	0.0479	0.0101	0.0407	0.0056	0.0305
Burpengary Creek	0.0637	0.1363	0.0186	0.0786	0.0167	0.0040	0.0159	0.0023	0.0135
Caboolture River	0.0128	0.0182	0.0034	0.0161	0.0037	0.0009	0.0043	0.0007	0.0039
Six Mile Creek	0.1252	0.2083	0.0327	0.1240	0.0248	0.0048	0.0209	0.0027	0.0137
Rose Creek	0.3753	0.8777	0.1120	0.4520	0.0865	0.0175	0.0739	0.0093	0.0485
Beerburum Creek 7a	0.5497	0.9915	0.1593	0.6270	0.1204	0.0141	0.0993	0.0130	0.0661
Tibrogargan Creek	0.2176	0.4597	0.0642	0.2481	0.0508	0.0046	0.0442	0.0057	0.0315
Coonowin Creek	0.0579	0.1121	0.0169	0.0687	0.0142	0.0025	0.0120	0.0017	0.0095
Coochin Creek	0.0457	0.0914	0.0132	0.0532	0.0111	0.0021	0.0116	0.0017	0.0091
Mellum Creek	0.0756	0.1665	0.0225	0.0971	0.0217	0.0053	0.0198	0.0026	0.0146
Mooloolah River	0.0374	0.0805	0.0118	0.0536	0.0130	0.0036	0.0133	0.0018	0.0102
Sippy Creek	0.1298	0.2985	0.0456	0.1984	0.0449	0.0110	0.0382	0.0048	0.0256
Beerburum Creek 1	1.1566	0.9229	0.2999	1.1429	0.2168	0.0090	0.1685	0.0228	0.1179
Beerburum Creek 2	0.8095	1.5189	0.2267	0.8892	0.1829	0.0147	0.1489	0.0202	0.1072
Beerburum Creek 3	0.5535	1.0137	0.1492	0.5774	0.1192	0.0118	0.0963	0.0132	0.0662
Beerburum Creek 4	0.3473	0.6206	0.0920	0.3576	0.0746	0.0074	0.0604	0.0079	0.0399
Beerburum Creek 5	0.4761	0.9302	0.1393	0.5593	0.1100	0.0118	0.0877	0.0114	0.0578
Beerburum Creek 6	0.3325	0.6382	0.1012	0.4027	0.0825	0.0089	0.0639	0.0082	0.0432
Beerburum Creek 7b	0.3989	0.7296	0.1073	0.4183	0.0824	0.0100	0.0654	0.0086	0.0458
Beerburum Creek 8	0.2871	0.5571	0.0852	0.3324	0.0708	0.0083	0.0531	0.0069	0.0375
Rose Creek 9	0.1699	0.4255	0.0547	0.2209	0.0460	0.0095	0.0349	0.0044	0.0220
Beerburum Creek 10	0.2787	0.5411	0.0827	0.3279	0.0678	0.0083	0.0516	0.0067	0.0357
Beerburum Creek 11	0.1902	0.3534	0.0588	0.2367	0.0494	0.0064	0.0375	0.0048	0.0253
Beerburum Creek 12	0.0872	0.1327	0.0183	0.0768	0.0142	0.0023	0.0127	0.0018	0.0087

Note the range in concentrations of the LREE (e.g., La) spans almost three orders of magnitude,

## East Queensland waterways

Y	Ho	Er	Tm	Yb	Lu	Mn	Zr	Filter type (microns)	pH	Salinity	Tempe- rature (°C)
0.0641	0.0026	0.0071	0.0010	0.0066	0.0010	8.6	0.107	0.45	7.30	0.137	18.4
0.0781	0.0031	0.0083	0.0012	0.0074	0.0012	7.6	0.153	0.45	7.69	0.164	16.4
0.1133	0.0042	0.0121	0.0019	0.0124	0.0020	6.6	0.220	0.45	6.69	0.059	22.6
0.1048	0.0042	0.0116	0.0018	0.0122	0.0021	52.4	0.256	0.45	7.47	0.071	18.4
0.0706	0.0026	0.0078	0.0012	0.0076	0.0012	26.7	0.128	0.45	6.73	0.067	20.9
0.0822	0.0033	0.0100	0.0017	0.0118	0.0020	25.3	0.092	0.45	6.99	0.065	19.5
0.0554	0.0022	0.0059	0.0008	0.0054	0.0009	8.4	0.086	0.22	7.30	0.137	18.4
0.0686	0.0027	0.0074	0.0010	0.0065	0.0011	7.6	0.116	0.22	7.69	0.164	16.4
0.1053	0.0038	0.0113	0.0018	0.0119	0.0019	6.1	0.180	0.22	6.69	0.059	22.6
0.0906	0.0036	0.0104	0.0016	0.0111	0.0019	51.1	0.211	0.22	7.47	0.071	18.4
0.0604	0.0023	0.0065	0.0011	0.0067	0.0011	25.5	0.088	0.22	6.73	0.067	20.9
0.0670	0.0027	0.0086	0.0014	0.0106	0.0018	24.7	0.067	0.22	6.99	0.065	19.5
0.1060	0.0038	0.0127	0.0025	0.0201	0.0039	166.8	0.045	0.22	6.97	0.390	16.0
0.0337	0.0010	0.0032	0.0005	0.0034	0.0006	73.1	0.035	0.22	7.37	0.274	18.4
0.0333	0.0008	0.0027	0.0004	0.0024	0.0004	475.4	0.018	0.22	7.19	3.698	17.0
0.1770	0.0062	0.0173	0.0025	0.0172	0.0029	115.3	0.316	0.22	6.48	0.243	15.4
0.0862	0.0029	0.0083	0.0013	0.0086	0.0014	185.9	0.256	0.22	7.04	0.388	14.6
0.0348	0.0010	0.0030	0.0005	0.0029	0.0005	25.7	0.051	0.22	7.43	0.225	20.0
0.0849	0.0029	0.0076	0.0011	0.0066	0.0011	16.4	0.269	0.22	7.30	0.122	16.6
0.2851	0.0092	0.0260	0.0039	0.0233	0.0037	53.0	0.951	0.22	5.92	0.103	15.9
0.3849	0.0126	0.0344	0.0048	0.0291	0.0047	35.9	1.264	0.22	6.01	0.128	15.7
0.1940	0.0061	0.0163	0.0023	0.0138	0.0021	132.9	0.692	0.22	6.42	0.078	15.9
0.0531	0.0018	0.0051	0.0008	0.0048	0.0008	48.0	0.177	0.22	6.67	0.098	16.5
0.0535	0.0017	0.0045	0.0006	0.0037	0.0005	41.5	0.074	0.22	6.74	0.085	16.7
0.0851	0.0031	0.0082	0.0012	0.0079	0.0013	212.5	0.135	0.22	7.13	0.300	15.1
0.0613	0.0021	0.0060	0.0008	0.0053	0.0009	94.8	0.102	0.22	7.32	0.227	15.8
0.1376	0.0049	0.0134	0.0019	0.0122	0.0019	73.2	0.202	0.22	6.34	0.088	15.8
0.6554	0.0231	0.0561	0.0077	0.0385	0.0025	3.9	1.623	0.22	5.88	0.062	14.3
0.5803	0.0215	0.0537	0.0077	0.0402	0.0038	829.8	1.553	0.22	5.91	0.289	14.0
0.3840	0.0134	0.0331	0.0048	0.0247	0.0021	275.7	1.217	0.22	6.09	0.157	13.2
0.2419	0.0081	0.0201	0.0029	0.0140	0.0011	205.9	0.498	0.22	6.05	0.172	12.8
0.3445	0.0119	0.0302	0.0044	0.0232	0.0028	283.3	0.737	0.22	5.82	0.139	13.6
0.2348	0.0086	0.0230	0.0032	0.0183	0.0022	80.4	0.735	0.22	5.71	0.112	14.1
0.2475	0.0090	0.0235	0.0033	0.0176	0.0020	27.1	0.732	0.22	6.05	0.120	14.6
0.1990	0.0072	0.0198	0.0028	0.0158	0.0020	30.9	0.209	0.22	5.84	0.110	14.2
0.1112	0.0043	0.0116	0.0016	0.0093	0.0009	31.0	0.591	0.22	5.68	0.108	14.6
0.1924	0.0071	0.0188	0.0027	0.0153	0.0021	32.5	0.621	0.22	5.78	0.099	14.3
0.1426	0.0051	0.0141	0.0021	0.0120	0.0017	19.7	0.396	0.22	5.92	0.101	15.2
0.0620	0.0020	0.0054	0.0008	0.0052	0.0011	59.8	0.151	0.22	6.37	4.119	16.9

whereas the HREE only span one order of magnitude.

calculated from  $\text{Pr}_n$  and  $\text{Nd}_n$  due to the possible overabundance of  $\text{La}_n$ . When calculating  $\text{Eu}^*$  we avoid  $\text{Gd}_n$  as it is often overabundant in seawater, and instead extrapolate from  $\text{Sm}_n$  and  $\text{Tb}_n$  or alternatively  $\text{Nd}_n$  and  $\text{Sm}_n$ . Similarly for  $\text{Gd}^*$ , we avoid  $\text{Eu}_n$  as it may be over- or underabundant, and extrapolate from  $\text{Sm}_n$  and  $\text{Tb}_n$  or alternatively,  $\text{Tb}_n$  and  $\text{Dy}_n$ .  $\text{Lu}^*$  is calculated from  $\text{Tm}_n$  and  $\text{Yb}_n$ . The extent of La, Gd and Lu anomalies is expected to be small but well beyond analytical uncertainty. The fundamental difference in electronic structure of these elements (and Y) compared to the other REEs (i.e. empty, half filled and completely filled f-orbitals) is a likely cause of differential behaviour and enhances the value of the REY as direct proxies for trans-uranic elements. Once appropriate neighbours have been identified for quantification of anomalies, two alternative methods for the actual calculation of  $\text{REE}_n^*$  are available.

In the majority of existing literature, anomalies are calculated on a linear scale (despite graphically illustrating the patterns on log-linear diagrams). Implicitly, in calculating anomalies with the linear method, we make the assumption that the difference in concentration between neighbouring pairs is constant. If this assumption holds, then graphically the REY pattern will behave linearly in the region of the near neighbours on a linear-linear plot. Anomalies from the most appropriate near neighbours using the linear method are expressed as follows:

$$\text{La}_n^* = \text{Pr}_n + 2 * (\text{Pr}_n - \text{Nd}_n) \quad (1)$$

$$\text{Ce}_n^* = \text{Pr}_n + (\text{Pr}_n - \text{Nd}_n) \quad (2)$$

$$\text{Eu}_n^* = 2/3\text{Sm}_n + 1/3\text{Tb}_n \quad (3a)$$

or

$$= 3/2\text{Sm}_n - 1/2\text{Nd}_n \quad (3b)$$

$$\text{Gd}_n^* = 2/3\text{Tb}_n + 1/3\text{Sm}_n \quad (4a)$$

or

$$= \text{Tb}_n + (\text{Tb}_n - \text{Dy}_n) \quad (4b)$$

$$\text{Lu}_n^* = \text{Yb}_n + (\text{Yb}_n - \text{Tm}_n) \quad (5)$$

Alternatively we can calculate the anomalies from a geometric average where the assumption is that the ratio between near neighbour concentrations is constant (McLennan, 1989). Graphically, the geometric assumption requires that the behaviour of near neighbours is linear on a log-linear plot. Anomalies calculated geometrically are obtained as follows:

$$\text{La}_n^* = \text{Pr}_n * (\text{Pr}_n/\text{Nd}_n)^2 \quad (6)$$

$$\text{Ce}_n^* = \text{Pr}_n * (\text{Pr}_n/\text{Nd}_n) \quad (7)$$

$$\text{Eu}_n^* = (\text{Sm}_n^2 * \text{Tb}_n)^{1/3} \quad (8a)$$

or

$$= \text{Sm}_n * (\text{Sm}_n/\text{Nd}_n)^{1/2} \quad (8b)$$

$$\text{Gd}_n^* = (\text{Tb}_n^2 * \text{Sm}_n)^{1/3} \quad (9a)$$

or

$$= \text{Tb}_n * (\text{Tb}_n/\text{Dy}_n) \quad (9b)$$

$$\text{Lu}_n^* = \text{Yb}_n * (\text{Yb}_n/\text{Tm}_n) \quad (10)$$

We inspected our data on both linear–linear and log–linear plots. Overall, the REY patterns behave more smoothly on log–linear plots. Therefore, the choice of a geometric calculation of REE\* is more appropriate for the present dataset. All anomalies were calculated using Equations (6)–(8a), (9a) and (10) and are presented in Table III. For 3 of the 19 samples (Mooloolah River, Sippy Creek and Mellum Creek), Equations (8b) and (9b) would probably be more appropriate than 8a and 9a due to the downward concavity of those specific REY patterns, where the point of inflection is centred near these elements. However, for ease of interpretation we applied only one set of equations to the entire dataset while noting that the Eu and Gd anomalies calculated for these particular samples are likely to be overestimates.

Either assumption (linear or geometric) appears to yield robust results for the Ce, Eu and Gd anomalies, where the differences in calculated anomalies for our samples are typically less than 2% (which is within the combined analytical errors). However, for the La anomaly the differences are as large as 30%. Ultimately, for samples that yield strongly curved overall REY patterns, it may be necessary to find a more appropriate normalising value (e.g. the suspended sediment from the river) before deciding between a linear and log–linear anomaly calculation. Indeed in some instances, anomalies can be artefacts of inappropriate normalisation (a source characteristic of the normalising values) and of no real geochemical significance. We tested the robustness of the anomalies calculated relative to MUQ by normalising with data provided by Kamber et al. (2005) for sediment from individual waterways (Tallebudgera Creek, North Pine and Caboolture Rivers), and with the widely applied PAAS average (Taylor and McLennan, 1985). It is clear that

Table III. Rare earth Element anomalies calculated following normalisation with MUQ (Kamber

	Geometric La Anomaly (equation 6)	Linear La Anomaly (equation 1)	Geometric Ce Anomaly (equation 7)	Linear Ce Anomaly (equation 2)	<i>Conventional Ce anomaly</i>	Geometric Eu Anomaly (equation 8a)
Coomera River b 0.45	1.234	1.369	0.885	0.911	0.763	0.855
Coomera River a 0.45	1.175	1.338	0.734	0.761	0.649	0.686
Nerang River b 0.45	1.148	1.197	0.757	0.766	0.687	0.898
Nerang River a 0.45	1.039	1.086	0.819	0.830	0.790	0.752
Tallebudgera Creek 0.45	1.061	1.085	0.851	0.857	0.815	0.816
Currumbin Creek 0.45	1.121	1.138	0.975	0.980	0.903	0.997
Coomera River b	1.225	1.320	0.844	0.863	0.734	0.856
Coomera River a	1.162	1.295	0.729	0.753	0.652	0.734
Nerang River b	1.234	1.336	0.770	0.789	0.666	0.886
Nerang River a	1.075	1.149	0.828	0.845	0.780	0.743
Tallebudgera Creek	1.107	1.157	0.877	0.889	0.815	0.838
Currumbin Creek	1.142	1.159	0.965	0.969	0.883	0.992
Cabbage Tree Creek	1.402	1.433	0.811	0.816	0.647	0.812
South Pine River	1.019	1.019	0.790	0.790	0.781	0.822
North Pine River	1.174	1.193	0.781	0.785	0.701	0.427
Little Burpengary Creek	1.049	1.087	1.036	1.047	0.996	0.992
Burpengary Creek	1.058	1.085	0.951	0.958	0.912	1.062
Caboolture River	1.437	1.695	0.769	0.805	0.601	1.017
Six Mile Creek	0.945	0.947	0.738	0.739	0.766	0.922
Rose Creek	0.939	0.943	0.968	0.969	1.006	0.977
Beerburum Creek 7a	0.920	0.920	0.750	0.750	0.791	0.563
Tibrogargan Creek	0.872	0.873	0.848	0.848	0.927	0.428
Coonowin Creek	0.972	0.977	0.824	0.825	0.837	0.811
Coochin Creek	0.961	0.964	0.851	0.852	0.872	0.830
Mellum Creek	1.073	1.115	0.975	0.987	0.924	1.124
Mooloolah River	1.116	1.226	0.943	0.970	0.865	1.244
Sippy Creek	0.926	0.970	0.871	0.883	0.899	1.183
Beerburum Creek 1	0.963	0.964	0.359	0.359	0.368	0.202
Beerburum Creek 2	0.945	0.945	0.804	0.804	0.834	0.385
Beerburum Creek 3	0.956	0.956	0.805	0.805	0.829	0.474
Beerburum Creek 4	0.980	0.980	0.802	0.802	0.813	0.480
Beerburum Creek 5	0.948	0.951	0.821	0.822	0.848	0.525
Beerburum Creek 6	0.895	0.897	0.768	0.769	0.824	0.533
Beerburum Creek 7b	0.971	0.971	0.811	0.811	0.827	0.593
Rose Creek 9	0.871	0.875	0.961	0.962	1.046	1.040
Beerburum Creek 8	0.883	0.883	0.781	0.781	0.847	0.588
Beerburum Creek 10	0.911	0.912	0.794	0.794	0.842	0.608
Beerburum Creek 11	0.900	0.903	0.739	0.740	0.789	0.650
Beerburum Creek 12	1.437	1.464	0.928	0.934	0.727	0.728

Linear and geometric anomalies are significantly different for La, but are similar for Ce, Gd and Eu. It is clear that the conventional method for calculating the cerium anomaly, (linear from La and Nd) Beerburum Creek 12 displays a large positive La anomaly (1.437), resulting in a deeply negative



et al., 2005)

Linear Eu Anomaly (equation 3a)	Geometric Eu Anomaly (equation 8b)	Geometric Gd Anomaly (equation 9a)	Linear Gd Anomaly (equation 4a)	Geometric Lu Anomaly (equation 10)	Linear Lu Anomaly (equation 5)	Y:Ho	Pr <sub>n</sub> /Yb <sub>n</sub>	Pr <sub>n</sub> /Tb <sub>n</sub>	Tb <sub>n</sub> /Yb <sub>n</sub>
0.855	0.812	1.117	1.117	0.950	0.950	24.25	0.872	0.799	1.092
0.684	0.620	1.069	1.067	1.068	1.069	25.34	0.614	0.555	1.106
0.898	0.867	1.053	1.052	1.056	1.056	27.04	0.595	0.750	0.794
0.752	0.703	1.123	1.122	1.065	1.067	25.05	0.629	0.706	0.890
0.815	0.790	1.039	1.038	1.056	1.057	26.95	0.900	1.005	0.896
0.996	0.978	1.074	1.073	0.994	1.005	25.13	0.694	1.008	0.688
0.856	0.792	1.128	1.127	1.044	1.044	25.46	0.870	0.801	1.086
0.732	0.683	1.111	1.107	1.088	1.089	25.76	0.585	0.553	1.057
0.886	0.856	1.095	1.094	1.015	1.016	27.43	0.541	0.724	0.748
0.742	0.686	1.065	1.064	1.082	1.085	24.85	0.595	0.657	0.906
0.837	0.814	1.073	1.071	1.061	1.061	26.28	0.853	1.012	0.843
0.991	0.975	1.060	1.059	0.985	1.003	24.56	0.637	1.016	0.627
0.811	0.775	1.052	1.050	1.021	1.063	28.21	0.426	1.040	0.409
0.822	0.809	1.087	1.087	1.107	1.111	32.68	0.793	1.001	0.793
0.427	0.386	1.181	1.181	1.282	1.283	39.97	0.653	0.802	0.814
0.987	0.913	1.061	1.055	1.039	1.043	28.70	1.169	1.102	1.061
1.062	1.033	1.073	1.073	0.995	1.000	29.80	0.833	0.958	0.870
1.013	1.036	1.101	1.096	1.125	1.125	33.94	0.447	0.612	0.731
0.914	0.857	1.100	1.090	1.147	1.153	29.60	1.914	1.423	1.345
0.968	0.927	1.121	1.110	1.107	1.111	31.12	1.845	1.406	1.312
0.558	0.534	1.081	1.070	1.127	1.132	30.51	2.104	1.434	1.467
0.425	0.397	1.117	1.108	1.082	1.087	31.77	1.781	1.326	1.342
0.808	0.771	1.024	1.020	1.083	1.083	28.78	1.353	1.152	1.174
0.830	0.848	1.088	1.087	0.988	0.988	30.84	1.357	0.916	1.482
1.121	1.028	1.104	1.101	1.062	1.062	27.86	1.098	0.997	1.102
1.244	1.148	1.131	1.131	1.101	1.101	28.63	0.858	0.760	1.129
1.172	1.032	1.119	1.108	1.006	1.006	27.89	1.433	1.106	1.295
0.200	0.191	1.036	1.024	1.106	1.112	28.39	2.530	1.538	1.645
0.383	0.356	1.050	1.041	1.100	1.105	27.02	1.907	1.312	1.454
0.471	0.438	1.039	1.031	1.108	1.114	28.73	2.016	1.319	1.528
0.475	0.435	1.073	1.061	1.181	1.197	30.03	2.145	1.358	1.579
0.519	0.486	1.071	1.058	1.171	1.176	28.96	2.023	1.424	1.421
0.525	0.475	1.076	1.059	1.038	1.038	27.35	1.891	1.452	1.302
0.587	0.549	1.064	1.051	1.096	1.097	27.58	2.057	1.461	1.408
1.022	0.910	1.078	1.058	0.992	0.992	25.80	1.984	1.454	1.364
0.578	0.510	1.056	1.037	1.061	1.061	27.81	1.864	1.453	1.283
0.599	0.540	1.059	1.042	1.105	1.106	27.19	1.868	1.444	1.293
0.640	0.572	1.064	1.046	1.056	1.056	27.75	1.713	1.429	1.199
0.726	0.740	1.053	1.051	1.245	1.245	31.74	1.305	1.197	1.091

The choice of normalising elements (i.e., equation 8a c.f. 8b)) sometimes has a greater impact. It is significantly different to anomalies calculated, more correctly, from Pr and Nd. specifically, Ce anomaly (0.727) which is in reality only slightly negative if calculated from Pr and Nd (~0.93).

whilst the magnitude of the La, Ce and Gd anomalies vary according to choice of normaliser, the features themselves clearly persist. The biggest deviations are found when comparing MUQ-normalised anomalies with those calculated using PAAS normalisation, probably due to slightly inaccurate PAAS Pr values (see Kamber et al., (2005) for a full discussion). The key point is that the anomalies are real, and not the result of inappropriate normalisation.

Some of the Eu anomalies in the studied stream waters change polarity when normalised with PAAS, a function of the stronger positive Eu anomaly present in the MUQ average. However, we still observe variability in Eu anomalies when PAAS normalising. Therefore, as long as one consistently uses the same normalising shale values for all samples, the relative differences in the Eu anomaly appear to have the potential to serve as provenance tracers.

## 5. Discussion

Before we consider the individual stream characteristics in detail, it is necessary to examine how our sample treatment may have influenced our results with respect to the initial creek water.

### 5.1. EVALUATION OF METHOD ON RESULTING REY CONCENTRATIONS

#### 5.1.1. *Effect of filtration*

Duplicate samples were taken from the Gold Coast region, with one aliquot filtered with 0.45  $\mu\text{m}$  filters, and the other with 0.22  $\mu\text{m}$  syringe filters in order to evaluate the effects of colloids that are not removed by filtration on the estimate of 'truly' dissolved REY because the difference between samples filtered with 0.45 and 0.22  $\mu\text{m}$  filters will simply reflect larger colloids. The effects of filtration are illustrated in Figure 4 where results for the 0.22  $\mu\text{m}$  are normalised to the 0.45  $\mu\text{m}$  filtrates. In general, the 0.22  $\mu\text{m}$  samples are between 5 and 15% lower in absolute REY concentration, with slight light to heavy fractionation induced by the smaller filtration diameter, an indication that the LREE are preferentially associated with colloids compared to HREEs, in agreement with previous studies (Sholkovitz, 1992; 1995). Figure 4 illustrates that the differential effects of the two filters is minor, and filtration alone does not enhance anomalous REY behaviour. On the basis of this observation all further samples were filtered with 0.22  $\mu\text{m}$  filters. The term 'dissolved REY' is thus here defined as all REY that pass through the employed filters, regardless of the actual physical speciation between truly dissolved, small particulate, and colloidal phases.

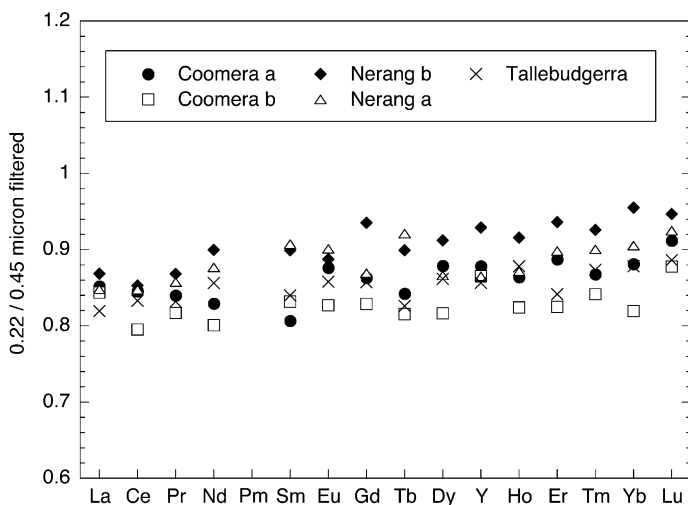


Figure 4. REY patterns for 0.22/0.45  $\mu\text{m}$  filtered samples. The flat patterns indicate that the anomalies (La, Ce, Eu, Gd, Y/Ho and Lu) are not related to differences in physical speciation attributable to the filtration protocol.

### 5.1.2. Effect of storage

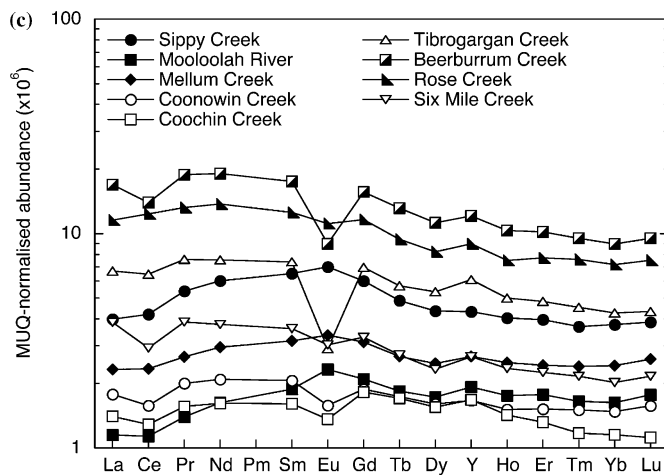
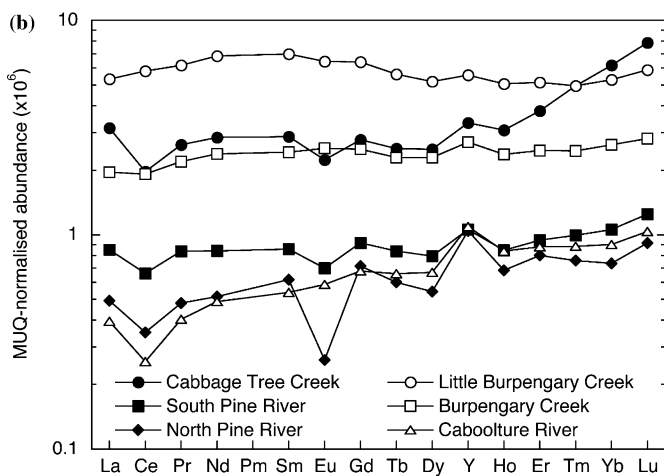
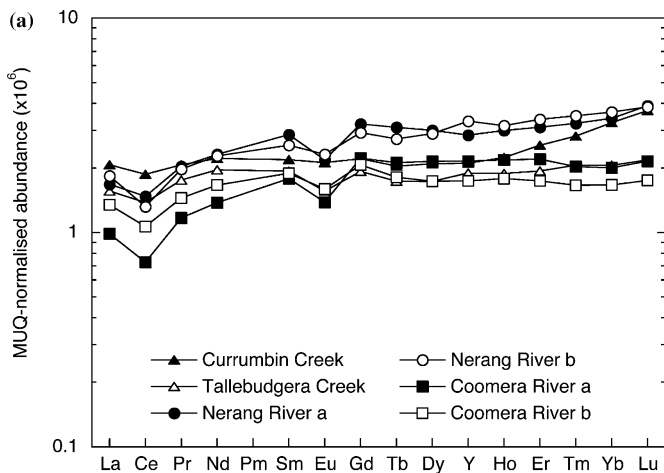
It is impossible to completely exclude the reactions occurring on the timescale between sampling and analysis (a maximum of 16 hours for this study). We reanalysed acidified samples that had been stored at room temperature for 14 days after sampling (all samples were acidified by the addition of  $\sim 120 \mu\text{L}$  of internal standard in 2% nitric acid immediately on return to the laboratory, lowering the pH to  $< 3$ ) and discovered, within analytical uncertainty, no changes in concentration or fractionation that would indicate either leaching of REYs from the centrifuge tube, or adsorption to the tube walls. We therefore assume that the short storage between sampling and analysis did not alter REY pattern.

## 5.2. ROBUST REY FEATURES IN STUDIED WATERS

MUQ normalised REY patterns of the streams are presented in Figure 5a–c, separated according to geographical location. Individual features of particular patterns are discussed below.

---

Figure 5. MUQ normalised REY patterns for SE Qld streams: Panel a: Gold Coast streams Panel b: Streams from Brisbane to Caboolture Panel c: Streams from Caboolture to the Sunshine Coast.



### 5.2.1. Total REY concentration and pattern shape: a reflection of pH?

The pH in the sampled streams ranges from 5.5 to 7.7 and there is a modest anticorrelation with total REY concentration (Figure 6a). This observation was first reported by Keasler and Loveland (1982) and has been repeatedly

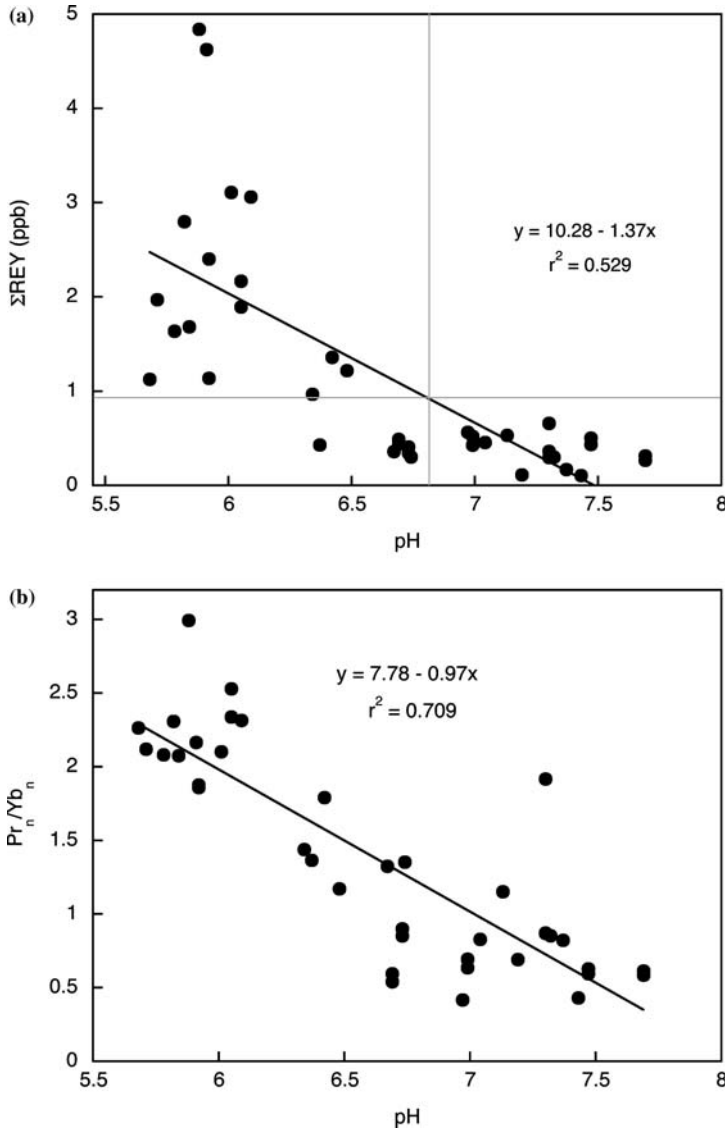


Figure 6. (a) Binary plot of the total REY (the sum of all REY) concentration against pH. The REY content of the samples is anticorrelated ( $r^2 = 0.529$ ) with pH. (b)  $\text{Pr}_n/\text{Yb}_n$  variation with pH (normalisation to MUQ). Values  $>1$  indicate that the light REE are enriched relative to the heavy REE, and values  $<1$  indicate heavy REE enrichment. The strong anticorrelation ( $r^2 = 0.709$ ) indicates that samples with lower pH are LREE enriched.

confirmed (e.g., Byrne and Sholkovitz, 1996). Elderfield et al. (1990) suggested that the pH effect may be the result of a general increase in the concentration of colloids low pH water.

In overall shape, our sediment-normalised REY patterns vary from slightly HREE enriched (as determined by the  $\text{Pr}_n/\text{Yb}_n$  ratio) in the lower total REY concentration streams to LREE and MREE enriched for the most concentrated samples. This change in REY pattern is at least partly driven by water pH as  $\text{Pr}_n/\text{Yb}_n$  ratios are significantly anticorrelated with pH (Figure 6b). This is a reflection of the solution chemistry of REY complexes (c.f. Goldstein and Jacobsen (1987) who observed that Sm/Nd ratios are correlated with pH). Byrne and Sholkovitz (1996; p. 529) suggested that the dependence of concentration and slope of REE pattern is 'mainly controlled by surface reactions where pH is a master variable in establishing the absolute and relative lanthanide abundance.'

Six Mile, Rose and Beerburrum Creeks (Figure 5c) are of interest as these they drain very similar lithological regions and form part of the upper catchment of Elimbah Creek. The pH of Rose and Beerburrum Creeks are the lowest of all creeks sampled at 5.92 and 5.68, respectively, and the REY concentrations are the highest (c.f. Six Mile Creek with a pH of 7.30). This is obviously not a function of the (identical) catchment geology, and we suggest that the differences are the result of differing land use in the respective areas of the catchment (Quinn and Stroud, 2002; Jennerjahn et al., 2004).

There are extensive pine plantations in the Rose and Beerburrum Creek catchments. A drop of pH is a typical water quality change in areas of conifer plantations where soils are poorly buffered (Friberg et al., 1998). If, as suggested by Friberg et al. (1998), the lowering of pH is a result of increased humic acid load from the breakdown of pine needles and bark, then the elevated REYs measured in our samples may simply reflect the expected high stability of REY-humic complexes in slightly acidic waters (Tang and Johannesson, 2003).

### 5.2.2. *Extent of LREE/HREE fractionation*

Notwithstanding the influence of pH on REY pattern slope, we observe a large variability in REY pattern shapes, evidently also in part reflecting different source lithologies such as the MREE-enriched (MUQ-normalised) Tertiary alkali basalts (with strong negative Eu anomalies) in the region.

Gold Coast streams (Fig 5a) are all broadly similar with low absolute REY concentrations, (La typically 50 ppt, Lu  $\sim$  1.5 ppt) with HREE enrichment ( $\text{Pr}_n/\text{Yb}_n$  varies from 0.54 to 0.9) and flat, moderately LREE depleted patterns.

Conversely, in Brisbane and Sunshine Coast streams, the  $\text{Pr}_n/\text{Yb}_n$  ratio varies from 0.43 (Cabbage Tree Creek) to  $\sim$ 3 in Beerburrum Creek, and absolute REY concentrations vary by orders of magnitude (Ce 25–1500 ppt

and Lu 0.4–4 ppt). The observation of LREE enrichment contrasts with the findings of Elderfield et al. (1990) who documented MREE and HREE but not LREE enrichments (defined in their case via  $La_n/Lu_n$ ) in river waters. The two waters in their dataset that are LREE enriched are the coarsely filtered (1  $\mu\text{m}$ ) Connecticut River samples. These LREE-enriched patterns were considered unrepresentative of the dissolved fraction, because they contain significant suspended particulate matter (probably LREE enriched). Whilst this explanation remains a possibility for the samples analysed by Elderfield et al. (1990) it does not apply to our samples that were filtered at 0.22  $\mu\text{m}$ . Hence, we regard the LREE enrichment shown by some of our stream waters as real.

Cabbage Tree Creek is distinct (Figure 5b) in that it shows a flat LREE to MREE pattern  $Pr_n/Tb_n \sim 1$ , but a significant MREE to HREE enrichment with a  $Tb_n/Yb_n$  ratio of 0.42. This creek is located in the most urbanised catchment of all the creeks studied, passing within 15 km of the centre of Brisbane, the largest population centre in Queensland. We are continuing to investigate whether urbanisation (or other land-use) could have affected this pattern.

Mellum Creek, Sippy Creek and the Mooloolah River (Figure 5c) show MREE enrichment with an overall concave profile centred on Sm with positive Eu and Gd anomalies. The MREE enriched patterns of these creeks is a common feature of phosphatic minerals and some rivers (Hannigan and Sholkovitz, 2001), and implies that the observed patterns may be due to the preferential weathering of phosphatic phases.

### 5.2.3. *La Anomaly*

A consistent feature of marine REY patterns is the strong positive La anomaly (Bau and Dulski, 1996; Zhang and Nozaki, 1996; Shields and Webb, 2004). Our samples show variable La anomalies that range from slightly negative in the high concentration Sunshine Coast streams, to moderately positive in the low concentration streams. We note that the anomaly is stronger in streams that have lower total REY concentrations (Figure 7) – which is itself related to pH. A possible explanation is that removal of LREE (presumably stronger in the REY poor waters) leads to the expression of a positive La anomaly even before reaching the estuarine trap. This behaviour may be related to the electronic structure of the  $La^{3+}$  ion, which has a noble gas configuration, and may behave more like a d-group than an f-group element.

However, the observed freshwater La anomalies are relatively small in comparison with that of seawater, where it averages 2.62 (an average of  $\sim 100$  MUQ-normalised values calculated from data published by Zhang and Nozaki (1996, 1998), Alibo and Nozaki (1999), Nozaki and Alibo (2003), using Equation (6)).

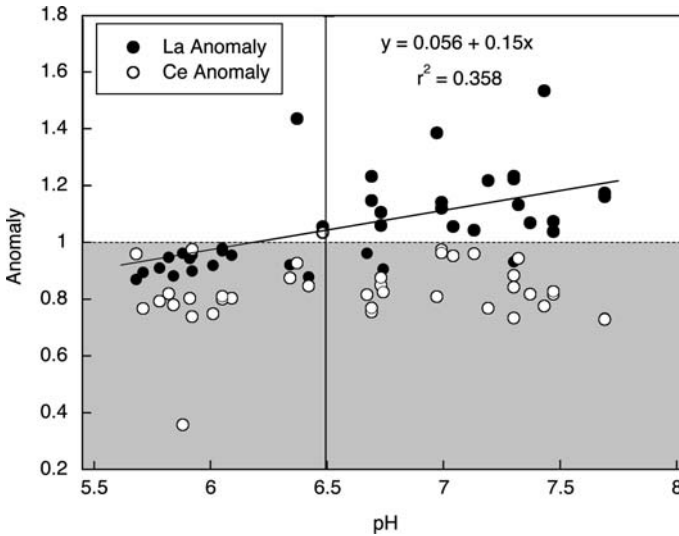


Figure 7. Comparison of geometric La and Ce anomalies (calculated using MUQ normalised Pr and Nd values) with pH. The La anomaly is correlated with pH ( $r^2 = 0.358$ ), whilst the Ce anomaly is pH invariant ( $r^2 < 0.1$ ). This observation contrasts with previous researchers who calculated the Ce anomaly using La and Nd values, and highlights the importance of choosing the most correct near-neighbours for anomaly calculations.

#### 5.2.4. Ce Anomaly

Negative Ce anomalies are a marine REY feature, but are also commonly observed in river waters (Sholkovitz, 1995; Byrne and Sholkovitz, 1996). Cerium has a redox potential between that of iron and manganese, such that oxidation from the dissolved  $\text{Ce}^{3+}$  ion to the virtually insoluble  $\text{Ce}^{4+}$  is expected to take place. Furthermore, (Moffett, 1990) showed that this reaction in seawater is biologically mediated and De Carlo et al. (1998) proposed that in strictly inorganic solutions, the Ce anomaly develops due to catalytic oxidative scavenging at fresh Mn-oxide surfaces. In contrast, despite being removed from solution in the presence of Fe-oxide surfaces, no anomaly develops due to this process (presumed to be an adsorption feature). Research on basalt weathering indicates that a negative cerium anomaly can develop in corestones due to differing mobility of Ce compared to other REY (Patino et al., 2003), implying that the negative Ce anomaly may also be a source characteristic with potential for providing provenance information. The Ce anomaly may therefore be related to weathering, inorganic aquatic processes, or biological mediation.

With the exception of Little Burpengary Creek, all the studied waterways exhibit negative Ce anomalies with an average value of 0.86. There is no correlation between the extent of Ce anomaly or between the concentrations of Mn and Ce (keeping in mind that variations in catchment geology would probably mask such a correlation).



The observed Ce anomalies are independent of pH (Figure 7), in contrast to some previously presented datasets (Goldstein and Jacobsen, 1988; Elderfield et al., 1990; Byrne and Sholkovitz, 1996). The largest negative Ce anomaly that we observe (0.36) actually occurs in one of the lower pH samples (pH = 5.88).

A possible explanation for this observation is that the cited studies calculated their Ce anomaly as a linear extrapolation between La and Nd (the closest available elements from isotope dilution methods), an approach that is naturally biased towards a large negative Ce anomaly due to the possible overabundance of La. For example, if we assume that Ce and Nd are strictly normally abundant (normalised values of 1), and that the normalised La value is 2.62 (the average seawater anomaly calculated in Section 5.2.3), then calculation of the 'conventional' Ce anomaly defined as  $Ce_n/Ce_n^* = 3 * Ce_n / (2La_n + Nd_n)$  results in an apparent, artificial Ce anomaly of 0.48.

Indeed, Figure 7 demonstrates that the extent of La overabundance increases with lower total REY concentration (partially related to increasing pH), which in turn results in the misinterpretation of an apparently stronger 'Ce anomaly' if calculated via La. It is therefore possible that at least some of the previously reported pH dependence of the negative Ce anomaly may in fact be due to a pH dependence of the undetected La anomaly. This requires further investigation with complete REE datasets.

### 5.2.5. *Gd Anomaly*

All streams have positive Gd anomalies that vary in magnitude from 1.02 in Cabbage Tree Creek to 1.18 in the North Pine River. Whilst the anomaly observed in the North Pine River (which has a slight saline influence) could be argued to be the result of mixing with seawater, we observe Gd anomalies between 1.08 and 1.12 in 14 separate, exclusively freshwater, samples. Previous workers have documented an anthropogenic origin for Gd anomalies (Bau and Dulski, 1996; Nozaki et al., 2000b), we have no reason to suspect, and no evidence to support, an artificial Gd source in our samples. Calculation of the Gd anomaly (relative to MUQ) for the ultrafiltered depth profiles presented in Alibo and Nozaki (1999) via Equation (9a), yields a range from 1.02 in the surface waters to a maximum of 1.22 in the intermediate water, with an average of 1.13. Some of our freshwaters have comparably large anomalies.

### 5.2.6. *Eu Anomalies*

Our dataset is characterised by strongly negative and strongly positive Eu anomalies for different samples (e.g., Tibrogargan Creek 0.42; Mooloolah River 1.15; using Equation (8b)). The negative Eu anomaly is a common feature of the Quaternary volcanics in the region, and indicates to some

extent the variable lithologies of the catchment. It is significant that the stream water patterns are not flat when normalised to the local volcanic REE patterns (Cohen, 2003), implying that weathering reactions of individual mineral phases and water pH are more important than bedrock characteristics in determining the aqueous REY pattern.

### 5.2.7. *Y/Ho Ratio*

Weight percent (unnormalised) Y/Ho ratios in our samples are variable. They range from the average upper continental crust and chondrite value of 26 (Kamber et al., 2005) to  $\sim 39$  indicating significant fractionation. The Y/Ho ratio of the Gold Coast samples is crustal, with values clustering between 25 and 27. Some Brisbane and Sunshine Coast samples show noticeable Y anomalies as evidenced by Y/Ho ratio greater than 27 for all samples with the exception of R-9 (Rose Creek). The two samples with highest salinity (North Pine River water, with a salinity of 3.698, Beerburrum Creek water Bb12 with a salinity of 4.119) have amongst the highest Y/Ho ratios (39 and 32). In these waters, the Y overabundance is likely due to admixing of seawater with a Y/Ho ratio of 55 (Nozaki et al., 1997; 2000a) or initial preferential HREE (relative to Y) loss in the estuarine trap.

However, in the Caboolture River, we found an Y/Ho ratio of 34, and a salinity of only 0.225. This river was sampled approximately 17 km upstream from its mouth *above* the Caboolture Weir, which physically prevents penetration of the salt wedge. In this sample, the elevated Y/Ho ratio is either an anthropogenic feature or was caused by freshwater fractionation.

## 5.3. DOWNSTREAM VARIATIONS IN REY BEHAVIOUR: THE EXAMPLE OF BEERBURRUM CREEK

Beerburrum Creek forms part of the upper catchment of Elimbah Creek along with the other tributaries, Six Mile Creek and Rose Creek. There are no published hydrological studies of this particular catchment but groundwater additions along the creeks (e.g., Bells Creek, at the Northern end of Pumicestone Passage; M. Cox, personal communication) are a well-known feature. Samples in Beerburrum Creek were taken on 16 June 2004. With the exception of one site (Bb-1), all samples represent the contiguous creek. There had been no rainfall recorded at the Beerburrum weather station in the previous 7 days, only 12.4 mm in the preceding 30 days, and 68 mm in the preceding 2 months. This compares to monthly long-term mean rainfall of 133.8 mm for May and 101.6 mm for June (Australian Bureau of Meteorology).

Beerburrum Creek is characterised by high total REY concentrations, with a strong LREE over HREE enrichment and a strongly negative Eu

anomaly. The total REY content is significantly correlated with Zr (Figure 8a), suggesting a terrigenous REY component, which itself implies that a substantial fraction of the REY are associated with a colloidal phase that passes through the 0.22  $\mu\text{m}$  filters. The colloidal phase is not correlated to Mn (Figure 8b), so the removal is not associated with Mn oxidation.

In general, individual REY concentrations decrease downstream with relative minima at Bb-4 and Bb-6 and relative maxima at Bb-5 and Bb-7a (Figure 8a). An interesting feature is the  $\sim 75\%$  apparent removal for all REYs from site Bb-2 to Bb-11 (samples with no estuarine influence) with the exception of Eu whose removal is  $\sim 55\%$ . Such extensive removal in freshwater has to our knowledge not previously been documented.

### 5.3.1. Coherence of REY

There is a surprisingly high level of coherence in the behaviour of the REY in Beerburrum Creek. There are strong linear correlations between individual REY concentrations, with correlation coefficients ( $r^2$ )  $> 0.96$  for all combinations with Sm including La, Gd, Y and Ho, except Ce (0.72) and Eu (0.45). Three samples deserve closer observation – Bb-1, R-9 and Bb-12. Rose Creek (R-9) is a different tributary that was analysed to investigate changes in pattern below the confluence of the two tributaries: Bb-1 is discontinuous from the main Beerburrum Creek due to low flow at the time of sampling and Bb-12 is the only sample with an estuarine influence. If we exclude these data points, correlation with Ce improves to 0.98 and that with Eu to 0.92.

The strong correlation between the REYs indicates that no significant fractionation is occurring between elements (with the exception of Eu), so that despite the large change in concentrations, the representative Beerburrum Creek REY pattern remains consistent. This is best appreciated in Figure 9 where MUQ normalised data are scaled to a constant total REY concentration.

The downstream concentration variation in Beerburrum Creek waters is caused by a combination of REY addition (from run-off and groundwaters with evidently similar REY patterns except for Eu) and REY removal occurring over the entire stream distance. The features of Beerburrum Creek are persistent temporally as well as spatially. Beerburrum Creek was sampled twice at location Bb-7, one month apart (Bb-7a and Bb-7b). While the absolute concentrations in the two waters vary, there is no variability in REY pattern over that sampling timescale.

*Ce anomaly.* As previously discussed in Section 5.2.4, cerium oxidation and precipitation is widely accepted as the mechanism for generating a negative Ce anomaly (Moffett, 1990; Alibo and Nozaki, 1999; Bau, 1999). Thus, one would expect that the Ce anomaly should deepen with distance downstream, but this is clearly not the case in Beerburrum Creek. For

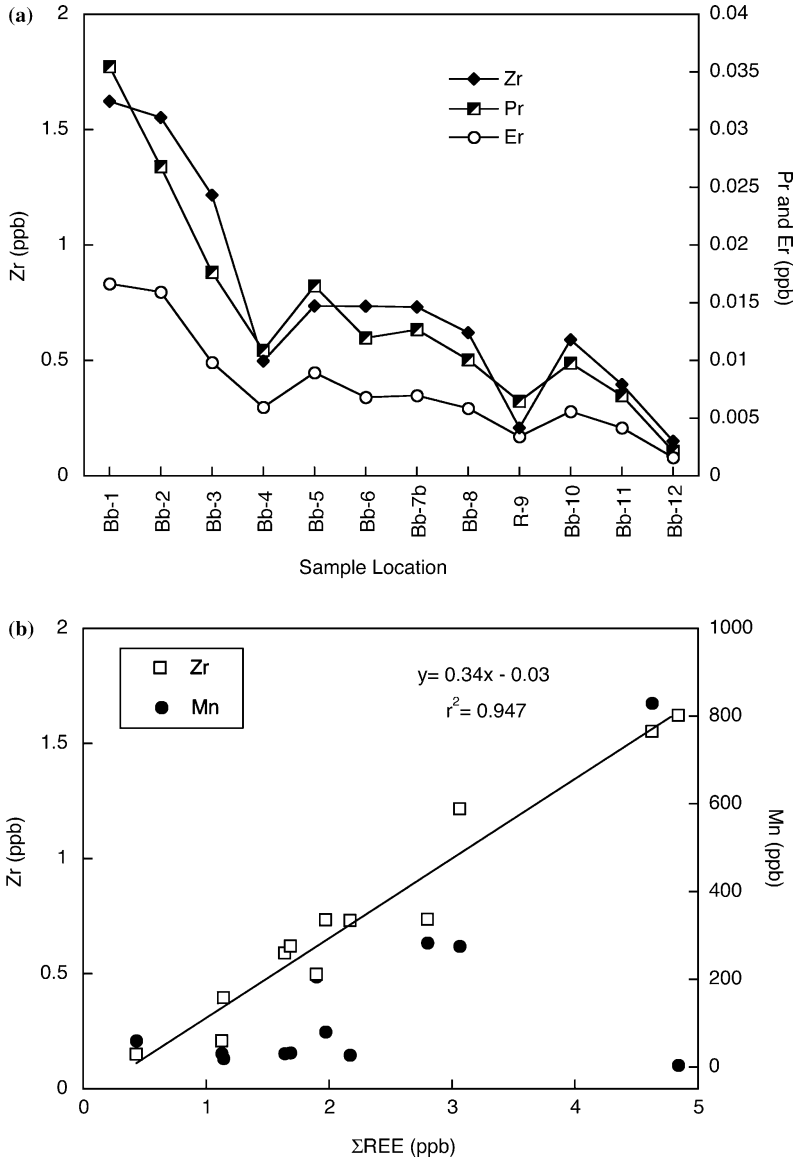


Figure 8. (a) Spatial variation of Zr, Pr and Er in Beerburrum Creek. Zr, a tracer of terrigenous particles is coherent with Pr and Er, chosen as representative light and heavy REY. The covariance indicates that the 'dissolved' REY load operationally defined by our filtration protocol ( $0.22 \mu\text{m}$  filtration) is strongly associated with colloidal particles. (b) Zr and Mn versus total REY concentration in Beerburrum Creek. Total REY is strongly correlated ( $r^2 = 0.947$ ) with Zr, indicating that the REY are transported in association with terrigenous particles that pass through our  $0.22 \mu\text{m}$  filters. There is no correlation with Mn, indicating that the removal behaviour of REY in Beerburrum Creek is controlled by coagulation of terrigenous particles, and is not due to oxidation of Mn.

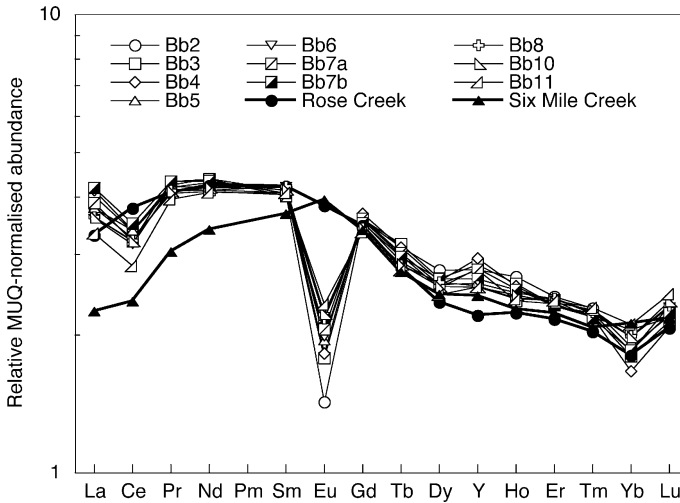


Figure 9. MUQ normalised Six Mile, Rose and Beerburrum Creek data scaled to same total REY concentration. This treatment of the dataset allows a comparison of the relative REY patterns. Whilst the Beerburrum Creek samples all display a similar pattern, this pattern is easily distinguished from that of the other tributaries within the catchment.

samples Bb2–Bb11, the correlation between  $Sm_n$  and  $Ce_n$  is almost perfect ( $r^2 > 0.99$ ). The removal from solution of 76% of the original Ce is completely coherent with the removal of the other REYs. As such, there is no need for an alternative explanation for the removal of Ce relative to its neighbouring REEs.

Thermodynamic calculations indicate that Ce oxidation is favoured under normal aquatic conditions (Akagi and Masuda, 1998), but comprehensive understanding of the weathering reactions of source bedrock and the subsequent transport of REYs appears critical to resolving the nature of freshwater Ce behaviour.

*Y/Ho fractionation.* In Beerburrum Creek, Y and Ho behave coherently, with no evidence for fractionation. This may suggest that the Caboolture River, which has a high Y/Ho ratio (34) might reflect an anthropogenic source (e.g., elevated Y/Ho is a feature of *marine* phosphate deposits, which are a major source of phosphate fertilisers (Hu et al., 1998)).

### 5.3.2. Eu Anomaly

The strongly negative Eu anomaly observed in Beerburrum Creek is also a feature of the Mt Beerburrum trachyte (0.73 relative to MUQ (Cohen, 2003)). However, even when we normalise the data to Mt Beerburrum whole rock data, we do not obtain a flat pattern or eliminate the negative Eu anomaly. This indicates that the aquatic REY patterns are not a direct

function of catchment geology, and are more likely the result of preferential weathering of separate constituents, such as friable glass in the dominant volcanic lithologies.

### 5.3.3. *Implications*

This is the first time that the REY pattern of a waterway has been shown to remain constant despite variations in total concentration. Comparison of the REY pattern of Rose and Six Mile Creek with those in Beerburrum Creek in Figure 9 demonstrates that the REY pattern of different tributaries within the same catchment can be distinguished on the basis of their relative REY pattern (i.e., neither Six Mile nor Rose Creek does display a negative Eu anomaly, and Six Mile Creek is LREE depleted relative to Beerburrum Creek). Hence, while the dissolved REY in a river may not correspond directly to the REY in the catchment lithology, the consistent REY pattern of a river can nonetheless be used as a provenancing tool.

Beerburrum Creek represents a small catchment characterised by low pH water, poor quality soils, low levels of phosphate and carbonate, and high dissolved organic matter (DOC). Accordingly, the likely REY speciation of Beerburrum Creek is not expected to be similar to large, slightly alkaline rivers such as the Mississippi River (Shiller, 1997; 2002) and our conclusions therefore are of relevance only to comparable catchments. In particular, we propose that in rivers (such as Beerburrum Creek) where REY speciation is largely organic (Tang and Johannesson, 2003), the potential for downstream coherence of REY is highest. This conclusion is supported by the findings of (Davranche et al., 2004), who found that removal of REY humic complexes with iron oxyhydroxides is not accompanied by fractionation.

## 6. Conclusions

We have demonstrated a method for successful quantification of REY concentrations in natural waters by ICP-MS, which uses calibration of instrument response to a dilute natural rock standard. This contrasts with previous methods that employed single or multi-element elemental calibration standards. Our results for the reference material SLRS-4 compare favourably with previously published results.

The REY profiles of 19 separate rivers and streams in SE Queensland are distinctive with respect to the overall shape of the REY patterns and to the extent of anomalies of individual elements. The variations in pattern appear to be the result of a combination of factors including source lithology, weathering and pH. In two particular catchments – Elimbah Creek and Mooloolah River – the differences in the REY pattern of different tributaries are not explained by differences in soil-type, lithology or different weather

patterns and are likely the result of differing land use (which results in a lowering of pH).

The down-stream study of Beerburrum Creek demonstrated, for the first time, significant coherent removal of up to 75% of the initial REY content in freshwater, without causing fractionation. For rivers with similar REY speciation as Beerburrum Creek, fingerprinting of freshwaters by REY pattern may become a provenance tool with potential to resolve environmental questions.

### Acknowledgements

The first author acknowledges financial support from ACQUIRE funds, an SPS PhD scholarship, and a Project AWARE Asia-Pacific micro-grant. This work benefited from access to a new quadrupole ICP-MS purchased from RIBG grant #120 4119 01 EMSP to the last author. The ACQUIRE clean-room facility was established by KDC with funds from the ARC and the University of Queensland. This manuscript was improved by the reviews of E.R. Sholkovitz and an anonymous reviewer.

### References

- Abal E.G., Dennison W.C. and Greenfield P.F. (2001) Managing the Brisbane River and Moreton Bay: an integrated research/management program to reduce impacts on an Australian estuary, *Water Science and Technology* **43**(9), 57–70.
- Akagi T. and Masuda A. (1998) A simple thermodynamic interpretation of Ce anomaly, *Geochemical Journal* **32**(5), 301–314.
- Alibo D.S. and Nozaki Y. (1999) Rare earth elements in seawater: Particle association, shale normalisation and Ce oxidation, *Geochimica et Cosmochimica Acta* **63**(3/4), 363–372.
- Aries S., Valladon M., Polve M., Dupre B. (2000) A routine method for oxide and hydroxide interference corrections in ICP-MS chemical analysis of environmental and geological samples. Geostandards Newsletter-the Journal of Geostandards and Geoanalysis.
- Astrom M. (2001) Abundance and fractionation patterns of rare earth elements in streams affected by acid sulphate soils, *Chemical Geology* **175**, 249–258.
- Baker J., Waight T. and Ulfbeck D. (2002) Rapid and highly reproducible analysis of rare earth elements by multiple collector inductively coupled plasma mass spectrometry, *Geochimica et Cosmochimica Acta* **66**(20), 3635–3646.
- Bau M. (1999) Scavenging of dissolved yttrium and rare earths by precipitating iron oxyhydroxide: Experimental evidence for Ce oxidation, Y–Ho fractionation, and the lanthanide tetrad effect, *Geochimica et Cosmochimica Acta* **63**(1), 67–77.
- Bau M. and Dulski P. (1996) Anthropogenic origin of positive gadolinium anomalies in river waters, *Earth and Planetary Science Letters* **143**, 245–255.
- Bolhar R., Kamber B.S., Moorbath S., Fedo C.M. and Whitehouse M.J. (2004) Characterisation of early Archean chemical sediments by trace element signatures, *Earth and Planetary Science Letters* **222**, 43–60.

- Byrne R.H. and Liu X. (1998) A coupled riverine-marine fractionation model for dissolved rare earths and yttrium, *Aquatic Geochemistry* **4**, 103–121.
- Byrne R.H., Sholkovitz E.R. (1996) Marine chemistry and geochemistry of the lanthanides. In: Gschneidner K.A. Jr, Eyring L. (eds) Handbook on the physics and chemistry of rare earths, Vol. 23, Elsevier. pp. 497–593.
- Cheatham M.M., Sangrey W.F. and White W.M. (1993) Sources of error in external calibration Icp-MS analysis of geological samples and an improved nonlinear drift correction procedure, *Spectrochimica Acta Part B – Atomic Spectroscopy* **48**(3), E487–E506.
- Cohen B.E. (2003) *Geochronology and Geochemistry of Southeast Queensland Tertiary Volcanism*. University of Queensland, Honours.
- Collerson K.D. (1995) Developments in radiogenic isotope geochemistry at the University of Queensland: Geochronological and geochemical applications. In: Johnson R.W., King C.R. (eds) Queensland: The State of Science. Royal Society of Queensland, pp. 305–337.
- Davranche M., Pourret O., Gruau G. and Dia A. (2004) Impact of humate complexation on the adsorption of REE onto Fe oxyhydroxide, *Journal of Colloid and Interface Science* **277**(2), 277–279.
- De Carlo E.H., Wen X.-I. and Irving M. (1998) The influence of redox reactions on the uptake of dissolved Ce by suspended Fe and Mn oxide particles, *Aquatic Geochemistry* **3**, 357–389.
- Eggin S.M., Woodhead J.D., Kinsley L.P.J., Mortimer G.E., Sylvester P., McCulloch M.T., Hergt J.M. and Handler M.R. (1997) A simple method for the precise determination of  $\geq 40$  trace elements in geological samples by ICPMS using enriched isotope internal standardisation, *Chemical Geology* **134**(4), 311–326.
- Elderfield H. (1988) The oceanic chemistry of the rare-earth elements, *Philosophical Transactions of the Royal Society of London, Series A* **325**, 105–126.
- Elderfield H., Upstill-Goddard R. and Sholkovitz E.R. (1990) The rare earth elements in rivers, estuaries, and coastal seas and their significance to the composition of ocean waters, *Geochimica et Cosmochimica Acta* **54**, 971–991.
- Friberg N., Rebsdorf A. and Larsen S.E. (1998) Effects of acidity and invertebrates in Danish streams and implications for freshwater communities in Denmark, *Water Air and Soil Pollution* **101**, 235–256.
- Goldberg E.D., Koide M., Schmitt R.A. and Smith R.H. (1963) Rare-earth distribution in the marine environment, *Journal of Geophysical Research* **68**, 4209–4217.
- Goldstein S.J. and Jacobsen S.B. (1987) The Nd and Sr Isotopic Systematics of River-Water Dissolved Material - Implications for the Sources of Nd and Sr in Seawater, *Chemical Geology* **66**(3–4), 245–272.
- Goldstein S.J. and Jacobsen S.B. (1988) Rare earth elements in river waters, *Earth and Planetary Science Letters* **89**, 35–47.
- Hannigan R.E. and Sholkovitz E.R. (2001) The development of middle rare earth element enrichments in freshwaters: Weathering of phosphate minerals, *Chemical Geology* **175**(3–4), 495–508.
- Hoyle J., Elderfield H., Gledhill M. and Greaves M. (1984) The behaviour of rare earth elements during mixing of river and sea waters, *Geochimica et Cosmochimica Acta* **48**, 143–149.
- Hu Y., Vanhaecke F., Moens L., Dams R., Del Castillo P. and Japenga J. (1998) Determination of the aqua regia soluble content of rare earth elements in fertilizer, animal fodder phosphate and manure samples using inductively coupled plasma mass spectrometry, *Analytica Chimica Acta* **373**(1), 95–105.
- Jennerjahn T.C., Ittekkot V., Klopper S., Adi S., Purwo Nugroho S., Sudiana N., Yusmal A., Gaye-Haake B. (2004) Biogeochemistry of a tropical river affected by human activities in



- its catchment: Brantas River estuary and coastal waters of Madura Strait, Java, Indonesia, *Estuarine, Coastal and Shelf Science* **60**, 503–514.
- Kamber B.S., Greig A. and Collerson K.D. (2005) A new estimate for the composition of weathered young upper continental crust from alluvial sediments, Queensland, Australia, *Geochimica et Cosmochimica Acta* **69**, 1041–1058.
- Kamber B.S. and Webb G.E. (2001) The geochemistry of late Archaean microbial carbonate: Implications for ocean chemistry and continental erosion history, *Geochimica Et Cosmochimica Acta* **65**(15), 2509–2525.
- Keasler K.M. and Loveland W.D. (1982) Rare-earth elemental concentrations in some Pacific Northwest Rivers, *Earth and Planetary Science Letters* **61**(1), 68–72.
- Lerche D. and Nozaki Y. (1998) Rare earth elements of sinking particulate matter in the Japan Trench, *Earth and Planetary Science Letters* **159**, 71–86.
- Masuda A. and Ikeuchi Y. (1979) Lanthanide Tetrad Effect Observed in Marine-Environment, *Geochemical Journal* **13**(1), 19–22.
- Masuda A. and Shimoda J. (1997) Depth profiles of lanthanide tetrad effect in the Western Indian Ocean and their implications, *Proceedings of the Japan Academy Series B – Physical and Biological Sciences* **73**(9), 187–191.
- McLennan S.M. (1989) Rare-earth elements in sedimentary-rocks – Influence of provenance and sedimentary processes, *Reviews in Mineralogy* **21**, 169–200.
- Moffett J.W. (1990) Microbially mediated cerium oxidation in sea water, *Nature* **345**, 421–423.
- Nelson B.J., Wood S.A. and Osiensky J.L. (2003) Partitioning of REE between solution and particulate matter in natural waters: A filtration study, *Journal of Solid State Chemistry* **171**, 51–56.
- Nothdurft L.D., Webb G.E. and Kamber B.S. (2004) Rare earth element geochemistry of Late Devonian reefal carbonates, Canning basin, Western Australia: Confirmation of a seawater REE proxy in ancient limestones, *Geochimica et Cosmochimica Acta* **68**(2), 263–283.
- Nozaki Y. and Alibo D.S. (2003) Importance of vertical geochemical processes in controlling the oceanic profiles of dissolved rare earth elements in the northeastern Indian Ocean, *Earth and Planetary Science Letters* **205**, 155–172.
- Nozaki Y., Lerche D., Alibo S.D. and Snidvongs A. (2000a) The estuarine geochemistry of rare earth elements and indium in the Chao Phraya River, Thailand, *Geochimica et Cosmochimica Acta* **64**(23), 3983–3994.
- Nozaki Y., Lerche D., Alibo S.D. and Tsutsumi M. (2000b) Dissolved indium and rare earth elements in three Japanese rivers and Tokyo Bay: Evidence for anthropogenic Gd and In, *Geochimica et Cosmochimica Acta* **64**(23), 3975–3982.
- Nozaki Y., Zhang J. and Amakawa H. (1997) The fractionation between Y and Ho in the marine environment, *Earth and Planetary Science Letters* **148**, 329–340.
- Patino L.C., Velbel M.A., Price J.R. and Wade J.A. (2003) Trace element mobility during spheroidal weathering of basalts and andesites in Hawaii and Guatemala, *Chemical Geology* **202**(3–4), 343–364.
- Piegras D.J. and Jacobsen S.B. (1992) The behaviour of rare earth elements in seawater: precise determination of variations in the North Pacific water column, *Geochimica et Cosmochimica Acta* **56**, 1851–1862.
- Quinn J.M. and Stroud M.J. (2002) Water quality and sediment and nutrient export from New Zealand hill-land catchments of contrasting land use, *New Zealand Journal of Marine and Freshwater Research* **36**, 409–429.
- Raczek I., Stoll B., Hofmann A.W. and Jochum K.P. (2001) High-precision trace element data for the USGS reference materials BCR-1, BCR-2, BHVO-1, BHVO-2, AGV-1, AGV-2, DTS-1, DTS-2, GSP-1 and GSP-2 by ID-TIMS and MIC-SSMS., *Geostandards Newsletter-the Journal of Geostandards and Geoanalysis* **25**(1), 77–86.

- Runnalls L.A. and Coleman M.L. (2003) record of natural and anthropogenic changes in reef environments (Barbados West Indies) using laser ablation ICP-MS and sclerochronology on coral cores, *Coral Reefs* **23**, 416–426.
- Shabani M.B., Akagi T., Shimizu H. and Masuda A. (1990) Determination of trace lanthanides and yttrium in seawater by inductively coupled plasma mass spectrometry after preconcentration with solvent and back extraction, *Analytical Chemistry* **62**, 2709–2714.
- Shields G.A. and Webb G.E. (2004) Has the REE composition of seawater changed over geological time, *Chemical Geology* **204**, 103–107.
- Shiller A.M. (1997) Dissolved trace elements in the Mississippi river: Seasonal, interannual, and decadal variability, *Geochimica et Cosmochimica Acta* **61**(20), 4321–4330.
- Shiller A.M. (2002) Seasonality of dissolved rare earth elements in the lower Mississippi River. *Geochemistry Geophysics Geosystems* **3**.
- Sholkovitz E.R. (1992) Chemical evolution of rare earth elements: Fractionation between colloidal and solution phases of filtered river water, *Earth and Planetary Science Letters* **114**, 77–84.
- Sholkovitz E.R. (1995) The aquatic chemistry of rare earth elements in rivers and estuaries, *Aquatic Geochemistry* **1**, 1–34.
- Sholkovitz E.R., Elderfield H., Szymczak R. and Casey K. (1999) Island weathering: River sources of rare earth elements to the Western Pacific Ocean, *Marine Chemistry* **68**, 39–57.
- Sholkovitz E.R., Piepgras D.J. and Jacobsen S.B. (1989) The pore water chemistry of rare earth elements in Buzzards Bay sediments, *Geochimica et Cosmochimica Acta* **53**, 2847–2856.
- Tang J. and Johannesson K.H. (2003) Speciation of rare earth elements in natural terrestrial waters: Assessing the role of dissolved organic matter from the modelling approach, *Geochimica et Cosmochimica Acta* **67**(13), 2321–2339.
- Taylor S.R., McLennan S.M. (1985) The continental crust: Its composition and evolution. *Geoscience Texts*, Blackwell.
- Van Kranendonk M.J., Webb G.E., Kamber B. and Pirajno F. (2003) Geological setting and biogenicity of 3.45 Ga stromatolitic cherts, east Pilbara, Australia, *Geochimica Et Cosmochimica Acta* **67**(18), A510–A510.
- Willmott W.F. (2004) Rocks and Landscapes of the National Parks of Southern Queensland. Geological Society of Australia, Queensland Division.
- Wyndham T., McCulloch M., Fallon S.J. and Alibert C. (2004) High-resolution records of rare earth elements in coastal seawater: Biogeochemical cycling and a new environmental proxy, *Geochimica et Cosmochimica Acta* **68**(9), 2067–2080.
- Yeghicheyan D., Carignan J., Valladon M., LeCoz B.M., Le Cornec F., Castrec-Rouelle M., Robert M., Aquilina L., Aubry E., Churlaud C., Dia A., Deberdt S., Dupre B., Freyrier R., Gruau G., Henin O., DeKersabiec M.A., Mace J., Marin L., Morin N., Petitjean P. and Serrat E. (2001) A compilation of silicon and thirty one trace elements measured in the natural river water reference material SLRS-4 (NRC-CNRC), *Geostandards Newsletter – the Journal of Geostandards and Geoanalysis* **25**(2–3), 465–474.
- Zhang J. and Nozaki Y. (1996) rare earth elements and yttrium in seawater: ICP-MS determinations in the East Caroline, Coral Sea, and South Fiji basins of the Western South Pacific Ocean, *Geochimica et Cosmochimica Acta* **60**(23), 4631–4644.
- Zhang J. and Nozaki Y. (1998) Behavior of rare earth elements in seawater at the ocean margin: A study along the slopes of the Sagami and Nankai troughs near Japan, *Geochimica et Cosmochimica Acta* **62**(8), 1307–1317.